

Isotopic study of geochemical evolution of fluid
with respect to carbonate chimney at the conical
seamount based on the mineral separation

メタデータ	言語: en 出版者: Shizuoka University 公開日: 2012-03-09 キーワード (Ja): キーワード (En): 作成者: Kato, Kazuhiro メールアドレス: 所属:
URL	https://doi.org/10.14945/00006444

理工学研究科;加

GD

K

0003503398

R

337

静岡大学附属図書館

THESIS

ISOTOPIC STUDY OF GEOCHEMICAL EVOLUTION OF FLUID WITH RESPECT
TO CARBONATE CHIMNEY AT THE CONICAL SEAMOUNT BASED ON THE
MINERAL SEPARATION

鉍物分離に基づく冷湧水起源の炭酸塩沈殿環境進化の同位体地球化学的研究

加藤和浩

静岡大学
大学院理工学研究科
環境科学専攻

平成 14 年 12 月



Abstract

Carbonates precipitated from the cold seepage are mainly composed of calcite, aragonite and dolomite. These minerals frequently coexist in same deposit. This occurrence suggests the different chemical condition during each mineral precipitation because simultaneous precipitation of carbonate minerals is unlikely from a single solution at any given physico-chemical condition. Although many isotopic studies for carbonates of cold seepage are carried out, isotopic analyses of individual minerals separated from coexisting condition is unperformed. The purpose on this study is to clarify the carbonate precipitation process by isotopic analyses based of coexisting carbonate minerals.

The sample is a carbonate chimney collected from the Conical Seamount at Mariana Forearc, composed of fine-grained calcite, aragonite, and an amorphous grain. Isotopic analyses of individual carbonate minerals of the carbonate deposits are key for understanding their formation. Calcite and aragonite were distinguished by staining using Meigen's solution, and isotopic composition was determined for both individual minerals. Remarkably contrasting isotope value in calcite and aragonite was revealed.

$\delta^{13}\text{C}$ value falls in a range from -0.48‰ to -2.12‰ , whereas $\delta^{18}\text{O}$ value falls in a range from $+4.20\text{‰}$ to $+6.71\text{‰}$. Especially, $\delta^{18}\text{O}$ value of the separated calcite and aragonite increased from the rim to the core of the chimney in cross section. Oxygen isotopic composition in each mineral of the rim part shows isotopic equilibrium with seawater. On the other hand, its composition of the core part shows an isotopic equilibrium with venting fluid squeezed from the serpentinite diapir below the Conical

Seamount.

The difference in ^{14}C activity ($\Delta^{14}\text{C}$) between calcite and aragonite, being from -975.8‰ (average) and -830.7‰ (average) for aragonite were observed. This result suggests the mixing of seawater and venting fluid during carbonate precipitation. ^{14}C activity suggests a different mixing ratio at each mineral precipitation. Aragonite was precipitated from the mixing fluid of 60% of seawater ($\Delta^{14}\text{C} = -240\text{‰}$) and 40% of venting fluid ($\Delta^{14}\text{C} = -1000\text{‰}$) and calcite was 90% of seawater and 10% of venting fluid. This result suggests different precipitation stage between calcite and aragonite in the chimney.

$^{87}\text{Sr}/^{86}\text{Sr}$ ratio in each mineral shows another view of carbonate precipitation in comparison with the result of ^{14}C activity. $^{87}\text{Sr}/^{86}\text{Sr}$ ratio of aragonite was 0.70914 (average) and calcite was 0.70674 (average). The mixing ratio of seawater ($^{87}\text{Sr}/^{86}\text{Sr} = 0.7092$) and venting fluid (estimated at $^{87}\text{Sr}/^{86}\text{Sr} = 0.7052$) calculated from $^{87}\text{Sr}/^{86}\text{Sr}$ ratio in calcite (10% of seawater, 90% of venting fluid) agree well with the result of ^{14}C activity. Whereas the mixing ratio for aragonite precipitation calculated from $^{87}\text{Sr}/^{86}\text{Sr}$ ratio shows 90% for seawater and 10% for venting fluid. The variation of calculated mixing ratio between ^{14}C activity and $^{87}\text{Sr}/^{86}\text{Sr}$ ratio at calcite precipitation is interpreted as a result of selective interpolation of seawater Sr during aragonite precipitation because strontium concentration of aragonite is about 10 times higher than that of calcite.

Isotopic analyses using the staining method is highly potential for isotopic study of carbonate deposits which are precipitated from the cold seepage. These deposits give us adequate data for understanding of mixing ratio between seawater and seepage fluid.

Carbonate deposits are composed of various carbonate minerals such as calcite, aragonite, and dolomite. In many cases, it is difficult to separate each mineral neither by microscopic observation nor by heavy liquid, because carbonate cementation is very fine. Staining methods will provide us pure mineral separates that can be utilized in deducing the evolution of carbonate rocks.

Contents

1. Introduction	1
1-1. Carbonate deposits related to cold seepage	1
1-2. Conical Seamount	2
1-3. Previous study of carbonate deposit of the Conical Cement	3
1-4. Objective of this study	4
2. Sample description	5
3. Method and procedure	6
3-1. Observation of mineral grains	6
3-2. Staining technique	6
3-3. Heavy liquid separation	8
3-4. X-ray diffraction	8
3-5. NIH Image 1.62f	9
3-6. Stable carbon and oxygen isotope ratios ($\delta^{13}\text{C}$ & $\delta^{18}\text{O}$)	10
3-7. Radiocarbon activity ($\Delta^{14}\text{C}$)	11
3-8. Strontium isotope ratio ($^{87}\text{Sr}/^{86}\text{Sr}$)	14
4. Results	15
4-1. Mineralogy of the Conical Seamount chimney	15
4-2. Mineral identification	17
4-3. Relative abundance of calcite and aragonite	19
4-4. Stable isotope measurements ($\delta^{13}\text{C}$ & $\delta^{18}\text{O}$)	20
4-5. Radiocarbon activity measurements ($\Delta^{14}\text{C}$)	21
4-6. Strontium isotope measurements ($^{87}\text{Sr}/^{86}\text{Sr}$)	22
5. Discussion	24
5-1. Carbonate chimney at the Conical Seamount, Mariana Forearc	24
5-1-1. Oxygen isotope	24
5-1-2. Radiocarbon activity	26
5-1-3. $^{87}\text{Sr}/^{86}\text{Sr}$ ratio	28
5-1-4. Precipitation of aragonite and calcite	30
5-1-5. Origin of carbon	33
5-2. Carbonate cement related to an old cold seepage	36
5-2-1. Konandai, Kanagawa	37
5-2-2. Shintomi town, Miyazaki	39
6. Summary	40
Acknowledgements	43
References	44

Contents

Figures

Figure 1: Index map of the Conical Seamount	50
Figure 2: Occurrence of chimney on the Conical Seamount	51
Figure 3: A horizontal cross cutting surface of chimney	52
Figure 4: Outline of vacuum glass line	53
Figure 5: Calibration curve for Sr concentration using ion-exchange resin	54
Figure 6: Grain shape and its color images taken by the microscope	55
Figure 7: SEM images forming the carbonate chimney	56
Figure 8: XRD results of bulk measurement and each grain shapes	57
Figure 9: Staining results of carbonate grains by using the Meigen's solution	58
Figure 10: Mineral separation results by using the Meigen's solution	59
Figure 11: Staining results of the thin section by using the Meigen's solution	60
Figure 12: Estimation curve for relative abundance of aragonite by using XRD	61
Figure 13: A horizontal cross cut surface of the carbonate chimney	62
Figure 14: Carbon and oxygen isotopic results of the carbonate chimney	63
Figure 15: Carbon and oxygen isotopic values of carbonates at Conical and Chamorro Seamount	64
Figure 16: Relationship between oxygen isotopic value and sampling loci	65
Figure 17: $^{14}\text{C}/^{12}\text{C}$ variation of standard sample (SRM-4990C) during September 2000 ~ October 2002	66
Figure 18: $^{87}\text{Sr}/^{86}\text{Sr}$ variation in seawater through a Phanerozoic	67
Figure 19: Mixing ratio of the seawater and the venting fluid at calcite and aragonite precipitation based on radiocarbon results	68
Figure 20: Bathymetry of the Conical Seamount with boring site of ODP leg125	69
Figure 21: Mixing ratio of the seawater and the venting fluid at calcite and aragonite precipitation based on the results of $^{87}\text{Sr}/^{86}\text{Sr}$ ratio	70
Figure 22: Relationship between polymorphism and magnesium concentration in solution	71
Figure 23: Chemical composition of pore water from cores at the Conical Seamount	72

Contents

Figure 24: A Bjerrum diagram	73
Figure 25: Relationship between methane index and carbon isotopic value	74
Figure 26: Compiled carbon and oxygen isotopic value of carbonates related to cold seepage	75
Figure 27: Index map of the locatin of boring site at Kounandai, Kanagawa	76
Figure 28: Detail topographic map of the boring site at Kounandai, Kanagawa	77
Figure 29: Cross section of the boring site at Kounandai, Kanagawa	78
Figure 30: Carbonate mineral assemblages of cementation and photo of core "D"	79
Figure 31: Carbon and oxygen isotopic results of core "D"	84
Figure 32: Index map of sampling location of carbonate cementation at Shintomi town, Kyusyu	85
Figure 33: Carbon and oxygen isotopic values of cementation collected from Kuge Shrine, Kyusyu	86

Tables

Table 1: All data for estimation of relative abundance of aragonite in the shimney	87
Table 2: All results of carbon and oxygen isotopic values of the chimney	89
Table 3: Radiocarbon activity of calcite and aragontie of the chimney	90
Table 4: Strontium isotopic results of calcite and aragonite of the chimney	91
Table 5: Strontium isotopic composition of modern seawater	92
Table 6: Composition of interstitial water, Site780 ODP leg125	93
Table 7: Isotopic difference between calcite and aragontie of the chimney	94
Table 8: Estimation of precipitation temperature and oxygen isotopic composition of the venting fluid	95
Table 9: Carbon and oxygen isotopic results of the cementation of Miyazaki	96

1. Introduction

1-1. Carbonate deposits related to cold seepage.

Cold seepage accompanying carbonate deposits distributes at plate convergent margins in the present ocean environment. Kulm et al. (1986) firstly reported the existent of carbonate deposits induced by cold seepage from Oregon subduction zone by using U.S. submersible "Alvin". In this area, June de Fuca plate subducts under the North America plate. According to Kulm et al. (1986), carbonate deposits and biotic community were observed in this area. Carbon isotopic compositions of carbonate deposits and molluscan tissues show negative values, being $-30\text{‰} \sim -50\text{‰}$ (Kulm et al., 1986) and this extremely negative isotopic values were clearly separated from other marine carbonate such as coral and foraminifera ($\sim 0\text{‰}$). Kulm et al. (1986) suggested the presence of carbonate ions depleted in ^{13}C as a carbon source and this carbonate ion was resulted from the methane oxidation by sulfate-reduction microbial activity. Carbonate deposits with negative carbon isotopic composition was also reported from Nankai Trough (Sakai et al., 1992), off Hatsushima Island (Hattori. et al 1994; Masuzawa et al., 1995), Kuroshima Knoll, Ryukyu Arc (Takeuchi et al., 2001), Monterey Canyon, CA (Stakes, 1999), Louisiana continental slope (i.e., Robert et al., 1990), North Sea (Hovland et al., 1987). Other carbonates with less negative carbon isotopic composition compared with methane-derived carbonates were reported from other cold seepage area; Otago continental slope, New Zealand ($\sim -10\text{‰}$, Orpin, 1997) and Conical Seamount ($\sim -1\text{‰}$, Haggerty, 1991), Mariana Forearc. Otago carbonate was precipitated from an aquifer-forced ground water (Orpin, 1997), whereas Mariana carbonate was precipitated

from the mixture of seawater and venting fluid originated from the deep-seated below the Conical Seamount (Haggerty, 1991).

According to the ancient cold seepage, many carbonate cements are found in various sedimentary strata on land. Direct estimation of the physico-chemical characteristics of such ancient cold seepages are difficult because it is impossible to obtain the formation fluids. Only detail isotopic and geochemical investigations of carbonate cements have a possibility for delineate the processes of the ancient cold seepages. It will be possible to clarify the ancient environmental change under the sea water and have a great potential for investigate the Earth's history such as the evolution of the sea water.

1-2. Conical Seamount

Conical Seamount is one of the serpentine mud volcanos located at Mariana Forearc. Similar kind of serpentine diapir developed in forearc region along Izu-Bonin-Mariana arc system and the serpentine was resulted from interaction between peridotite and fluid derived from subducted slab (Fryer et al., 1990).

Many previous studies in this area have been carried out with respect to geological process on geochemical cycling at convergent margins, and seismicity within subduction zone reviewed by Fryer (1996). According to Fryer (1996), fault system was developed at Mariana Forearc due to subducting Pacific plate, and distribution of serpentinite seamounts were controlled by these fault system. Seamounts are arranged parallel to the trench axis and development of accretionary prism is less in Mariana Forearc.

Serpentinite were resulted from the interaction with mantle peridotite and slab-derived fluid in mantle wedge. Serpentinite seamounts were resulted from the intrusion of deep-seated serpentinite along fault system. Conical Seamount is the one of the serpentine diapirs developed at Mariana forearc and it is located near a large graben in the outer forearc and its diapir basement located at 4200m deep at 19°32'N, 146°40'E (Figure 1), and its elevation is about 1000m from the basement (Fryer et al., 1990).

Carbonate deposit showing cylindrical shape was first discovered at the summit of Conical Seamount during the first investigation with submersible "Alvin" in 1987 and carbonate chimney was collected during a series of this dive. The chimney was composed of calcite and aragonite as carbonate phases (Haggerty & Cloutier, 1988). At the present-day Pacific Ocean, aragonite compensation depth (ACD) is as shallow as 2000m (Scholle et al., 1983). Aragonite in chimney shows a specific occurrence because aragonite is presence in deeper water depth (3,100m) than ACD. A conduit structure interpreted as a canal for fluid flow was observed at the lower part of the carbonate chimney and textural property of the upper part of the chimney was described as friable and porous (Haggerty, 1991).

Previous isotopic studies of carbonate chimney had been carried out by Haggerty (1991). After five years, the dive expedition using Japanese submersible "Shinkai 6500" was carried out in the Mariana Forearc region. A carbonate chimney in this study was collected from the summit of the Conical Seamount during #179 dive of "Shinkai 6500" (Fujioka et al, 1994).

1-3. Previous study of carbonate deposit of Conical Seamount

Previous studies related to carbonate sediments of the Conical Seamount were reported by Haggerty (1987). Radial acicular bundles of aragonite needles and Mg-calcite deposits in the sediment were collected by dredge samples. Carbon isotopic composition of these carbonates showed negative value ranged from -9.0‰ to -21.2‰ in comparison with the normal marine carbonate isotopic value ($0\text{‰} \sim +2\text{‰}$). Haggerty (1987) suggested that several possible carbon sources such as oxidizing methane or carbon dioxide from reaction with serpentinized ultra-mafic rocks, dewatering subducting slab, and oxidized organic hydrocarbon.

Isotopic composition of carbonate chimney which was collected by "Alvin" in 1987 fall range from -0.1‰ to -2.9‰ for carbon isotope and fall range from 5.0‰ to 5.8‰ for oxygen isotope (Haggerty 1991). Haggerty (1991) summarized that possible carbon source with negative carbon isotopic composition is methane in the venting fluid because geochemical study during ODP leg 125 detected methane presence in the pore water collected from drill core (Mottl, 1992).

1-4. Objective of this study

In the present marine environment, inorganic marine carbonate deposits are found at the cold seepage or venting fluid area such as carbonate chimneys on Conical Seamount, Mariana. These carbonate deposits have resulted from dynamic chemical change due to the mixing of seawater and venting fluid beneath the seafloor. The fluid variety is classified into three types based on their geological settings, altered seawater

resulted from the interaction of seawater and oceanic crust, methane gas hydrate including biogenic and thermogenic methane and petroleum, and the fluid origin from groundwater. These deposits are mostly composed of multi phase of carbonates such as calcite, aragonite, and dolomite. Although a large number of studies have been carried out on carbonate deposits regarding venting fluids in the present and fossil seepages, little is known about isotope analyses based on individual carbonate mineral separated from the mixed carbonates. The isotopic study of carbonate deposits composed of a couple of carbonate minerals should initially separate the individual minerals because coprecipitation of multi-mineral phases from a single solution is unlikely at any given physicochemical condition. In previous studies, thus, have summarized a model which resulted from mixing of the ambient seawater and venting fluids and have not been able to designate the mixing process of two fluids during carbonate precipitation. The fundamental aim of this study is to focus on geochemical understanding on the evolution of a cold seepage based on a mineral separation for isotopic analyses ($\delta^{13}\text{C}$, $\delta^{18}\text{O}$, ^{14}C , and $^{87}\text{Sr}/^{86}\text{Sr}$) of carbonate chimney composed of calcite and aragonite collected from the Conical Seamount, Maiana. Such a specific technique will provide us a wide application for investigation on the ancient carbonate cements.

2. Sample description

The sample for this study was collected near the top of the Conical seamount by "Shinkai 6500" at 3147m of water depth (Fujioka et al., 1994). The original size of the carbonate chimney was with ca. 2m in height and ca. 30cm in diameter at its root and was slightly

tilted (Figure 2). The sample was collected from the upper part of chimney and its shape was near conical. The wet weight of the sample was 12kg and the size was 40cm in height and 25cm x 15cm in major and in minor axis respectively, just after collected by "Shinkai 6500". Figure 3 shows a cut surface of the collected carbonate chimney soon after its sampling picture was taken on "R/V Yokosuka" during a series of dive expedition of "Shinkai 6500". This carbonate chimney did not show any conduit structure for the canal of fluid such as observed in sulfide chimneys which were vigorously discharging black smoker. The sample was porous and poorly cemented and so fragile that it could even be easily broken by hand. The color was mostly white and no detrital fragments such as serpentine mud distributed around the chimney was not included in the collected sample. Although a typical conduit structure was absent in our sample, this sample is also a "chimney" since the texture of our sample is analogous to the inside structure of upper part of the other chimney.

3. Method and Procedure

3-1. Observation of mineral grains

The grain shape of the mineral phase in the chimney was observed by the microscope and Scanning Electron Microscope (SEM) housed in Shizuoka University in order to identify carbonate mineral phase based on its grain shape. The grain size for SEM observation was sieved in range from 125 μ m to 250 μ m.

3-2. Staining technique

Staining technique using the Alizarin red solution, Feigl's solution, and Meigen's solution was applied to distinguish aragonite from the coexisting calcite. Hutchison (1974) reviewed staining methods for carbonate minerals: Alizarin red is used to distinguish calcite and aragonite from other carbonates. Feigl's and Meigen's solutions are used to identify aragonite from other carbonate minerals. The usage of Meigen's solution was formerly introduced as a technique of aragonite identification by Holmes (1921). Recently, treatment with Meigen's solution to differentiate between aragonite and calcite identification was applied to the observation of molluscan shell microstructure by Suzuki et al. (1993). They reported that this staining method has an advantage for the ultra microscale structure with fossil molluscan shells by energy dispersive x-ray spectrometry EDS because the staining aragonite surface contains a cobalt signature from Meigen's solution.

Meigen's solution was prepared using the following method introduced by Suzuki et al. (1993). A commercial reagent of cobalt nitrate, $\text{Co}(\text{NO}_3)_2 \cdot 6\text{H}_2\text{O}$, was dissolved in distilled water at a concentration of 10wt% in the solution. Several milliliters of Meigen's solution was placed into a small beaker or schale and then the carbonate grains that were crushed and sieved at $125\mu\text{m}$ to $250\mu\text{m}$ were immersed into the solution. The temperature of Meigen's staining solution and the carbonate grains were kept constant at 70°C in an oil bath for 15 minutes. After 15 minutes, the carbonate grains were filtered off and gently washed with distilled water (Kato and Wada, 2001). The aragonite crystal surface changed color from white to purple, while the calcite did not change during this treatment. Temperatures and staining time that were the most efficient in

distinguishing aragonite were determined after several trial experiments. Feigl's solution was prepared by the following procedure: a mixture solution of silver sulfate and manganese sulfate was boiled and then after cooling, sodium hydroxide solution was added to this solution (Hutchison, 1974). Staining was carried out in room temperature. The sample was immersed in Feigl's solution and aragonite surface color changed from white to black gradually with time, staining time was approximately 10 minutes.

3-3. Heavy liquid separation

A heavy liquid of sodium polytungstate (SPT) which is a commercial reagent provided by SOMETU in Germany was attempted to separate individual mineral from calcite and aragonite mixtures. SPT is the most safest of all the heavy liquids because the toxicity of SPT has not been reported. SPT, $3\text{Na}_2\text{WO}_4 \cdot 9\text{WO}_3 \cdot \text{H}_2\text{O}$ in a chemical formula, is a noncombustible, smell-less, stable and neutral in the solvent pH range from 2 to 14. Specific gravity can be adapted range from 1.0 to 3.1g/cc in continuously and maximum value is 3.11g/cc (Danbara et al., 1992). A specific gravity of SPT was adjusted using the relationship between density and concentration of SPT reported by SOMETU, and an accurate density of SPT solution was checked by an archimedes' principle and glass densimeter and solution density was adjusted at 2.9, since specific gravity of calcite and aragonite was approximately 2.7102 and 2.947, respectively.

3-4. X-ray diffraction

X-ray diffractometer (XRD) of RIGAKU, RINT-2200, installed at Shizuoka

University was used to check carbonate mineral phase of chimney and estimate relative abundance of calcite and aragonite in the chimney.

Mineralogy was determined by using the characteristic X-ray of $\text{CuK}\alpha$ induced by energized 40kV and 20mA. Scan speed and step were 1° per minute and 0.01° per step, respectively. The bulk measurement was carried out in order to identify the mineral composition of chimney. The relative abundance of calcite and aragonite from the mixture was estimated using the calibration curve corrected by measurements of the standard sample which was an adjusted to the known calcite and aragonite ratio.

The calibration line used in this estimation was the principle peaks of aragonite, 3.40\AA (2θ , $\text{CuK}\alpha = 26.2^\circ$), and calcite, 3.03\AA (2θ , $\text{CuK}\alpha = 29.4^\circ$) because they had the greatest intensity for aragonite and calcite and were relatively free of interference from peaks between aragonite and calcite. The intensity ratio in the mixture of calcite and aragonite was measured in each weight percentage. The sample used for making this calibration was a bivalve fossil for aragonite and a metamorphic calcite collected from Tojyo, Hiroshima Prefecture. The weight of calcite and aragonite mixture was adjusted in 0.04g, and a repeat measurement was carried out ten times for reproducibility in the same weight ratio. Peak intensity of calcite and aragonite which was listed in Table 1 included error of 10.2% in maximum.

3-5. NIH Image 1.62f

NIH Image 1.62f was used for cross check of relative abundance of calcite and aragonite estimated by XRD. This software was image processing and analyses

software and was possible to download in free from internet web page at <http://rsb.info.gov.nih-image/Default.html>. This software was possible to calculate the dimension arbitrarily assigned part in the picture. In this study this software was attempted to estimate the relative abundance of calcite and aragonite in chimney, and the exemplum method of this estimation using Macintosh was shown in the followings.

The image of thin section stained by Meigen's solution was captured by using a digital microscope of KEYENCE, VH-6300. The thin section and a scale according as magnification for observation was saved as "JPEG" file in a floppy disk. Calcite and aragonite in the captured picture was discretely dyed in black color by using "Adobe Photoshop" and the dyed picture in each mineral was separately saved in pict format file. A color mode of NIH was changed to gray scale black color area assigned by photoshop in each mineral was automatically recognized as the distribution part of calcite or aragonite in a worked image and calculated to dimension in mm² scale using the original scale size. The calculated distribution dimension of calcite and aragonite in the same thin section considered as a relative abundance of calcite and aragonite in the chimney.

3-6. Stable carbon and oxygen isotope ratios($\delta^{13}\text{C}$ & $\delta^{18}\text{O}$)

Carbon and oxygen isotopic measurements were carried out with a MAT 250 at Shizuoka University. Carbonate sample less than a hundred micrograms was decomposed to carbon dioxide reacted with concentrated phosphoric acid at 60.00°C in high vacuum. Carbonate reaction vessel was connected to mass spectrometer and carbon dioxide reacted in this vessel was directly analyzed for stable isotope of carbon

and oxygen (Wada et al., 1982; Wada et al., 1984). The sample amount for measurement was sufficient in less than 100 μ g. The isotopic values of carbonate were given in a conventional notation with respect to PDB (PeeDee belemnite standard). Reproducibility of isotopic analysis was $\pm 0.02\%$ for carbon and $\pm 0.04\%$ for oxygen isotopic value and this value was obtained from the measurement of the laboratory reference gas called as "machine standard" which was released from the Solnhofen limestone by reaction with conc. phosphoric acid. SMOW scale of oxygen isotopic value was converted from the oxygen isotopic value in PDB scale by using the equation given by Friedman and O'Neil (1977) as:

$$\delta^{18}\text{O}_{\text{SMOW}} = 1.03086 \delta^{18}\text{O}_{\text{PDB}} + 30.86$$

3-7. Radiocarbon activity ($\Delta^{14}\text{C}$)

Radiocarbon analysis was carried out by liquid scintillation counting (LSC) and accelerator mass spectrometry (AMS). About 20g of chimney fragment containing calcite and aragonite was used to synthesize benzene, which was used for ^{14}C activity measurement of the bulk chimney carbonate by LSC at Radiochemistry Laboratory, Shizuoka University. The chimney fragment was reacted with hypochlorous acid, and released carbon dioxide was cryogenically purified. Acetylene and benzene were synthesized in stepwise from carbon dioxide in a vacuum line based on the introduced method by Fukuhara et al. (1995) and Takahashi and Wada (1998).

Radiocarbon activities in calcite and aragonite were measured by the MALT (Micro Analysis Laboratory, Tandem accelerator) of AMS at the University of Tokyo (Kobayashi

et al., 2000). For AMS measurements, about 10mg of each mineral was collected by hand picking from stained chimney fragments (see chapter 3-2). Separated and purified calcite and aragonite were reacted with concentrated pyro-phosphoric acid. Carbon dioxide released in vacuum line was cryogenically purified as shown in Tsuchiya and Wada (2002). Figure 4 shows the outline of glass vacuum line and it is composed of four functional parts as follows; the reaction vessel, cryogenic purification, gas volume measurement part, and sealing part. This line was pumped out by the turbo molecular pump and actualizes oil-free and high vacuum, and optimized to sample preparation for radiocarbon analyses. Carbonate sample and magnetic stirrer put into reaction vessel and reaction vessel was capped with silicon septum and then this vessel was connected to glass line. For evacuate reaction vessel, valve 14 in Figure 4 was slowly opened and evacuate the reaction vessel. When vacuum gauge in the reaction vessel reach at high vacuum lower than 10^{-1} Pascal, digital manometer displays -760mmHg and then reaction vessel was isolated by closing valve 14 for reaction. To decompose the carbonate mineral in to carbon dioxide, about 5ml pyro-phosphoric acid solution (ca. 87%) put into the reaction by penetrating the silicon septum by needled syringe. Although it takes long time up to a few hours for completiny the reaction in room temperature, the reaction rate was accelerated by heating using hair drier and reaction time was decreased to about half an hour. After reaction, carbon dioxide was cryogenically purified thorough the purification part vacuum line. The gas filled in the reaction vessel was mainly composed of carbon dioxide and water vapor. Carbon dioxide was separated by cryogenic distillation. After *n*-pentane - liquid nitrogen refrigerant (-130°C) was set to

T4 and liquid nitrogen (-196°C) was set to T3, the gas was expanded between valve 11 in Figure 4. The water vapor was trapped in T4 and carbon dioxide was trapped in T3 through T4. For determination of gas volume, carbon dioxide trapped in T3 was moved to gas volume measurement line in Figure 4. Carbon dioxide was moved from T3 to T2 in the following procedure: liquid nitrogen was set to T2 and then open valve 11 and remove liquid nitrogen of T3. The gas volume of carbon dioxide was measured by using mercury manometer in the red color space in Figure 4. Carbon dioxide was moved to sealing part and sample gas was preserved in the sealing tube (6ϕ pyrex tube). The sealed carbon dioxide was introduced to reaction vessel for graphitization from the sealing part. Flexible tube was attached to the end of glass line at valve 10 using ultra-torr joint and sealed tube was set in this flexible tube. The graphitization unit was attached at end of glass line at valve 14 using ultra-torr joint. Reaction vessel composed in reaction unit was 9ϕ vycor tube. The tube was preheated at 700°C to remove carbon source different from the samples. The iron powder of graphitization catalysis was in advance put into in the reaction vessel. To remove any contamination material adhered on iron powder, reaction vessel was pre-heated at 650°C filled with ultra pure hydrogen about one atmosphere about one hour. After sufficiently reduction on metal iron in the reaction vessel, filled hydrogen gas in the reaction vessel was pumped out and then liquid nitrogen was set to T0. The sample gas in sealed tube was cracked using Cajon flexible tube cracker and then carbon dioxide was expanded in the glass line and trapped it to T0 by liquid nitrogen. After carbon dioxide was completely trapped at T0, ultra pure hydrogen gas was introduced into the reaction line at approximately 80 kPa and was

isolated from glass line by closing valve 0. The liquid nitrogen trap of T0 was exchanged to *n*-pentane - liquid nitrogen trap for advancing the reduction of carbon dioxide. It will take about two hours for complete reaction. This procedure is modified from the batch preparation method reported by Kitagawa et al. (1993).

The amount of graphite transformed from 10mg carbonate was recovered 0.6mg to 1.2mg and the yield of graphite from carbon dioxide was approximately 70% (Tsuchiya and Wada, 2002). The oxalic acid provided from the National Institute of Standard and Technology (NIST) was used for an international standard sample of SRM-4990C. The radiocarbon activity in the atmosphere in 1950 A.D. which corresponded to the reference of radiocarbon measurement was defined by the measurement of this standard sample. Radiocarbon activity in the atmosphere in the reference was equal to 74.59 percent of the activity of the oxalic acid standard which was corrected for carbon isotopic fractionation to the reference value of $\delta^{13}\text{C} = -25\%$. $\Delta^{14}\text{C}$ value in the samples denote the per mil deviation of $^{14}\text{C}/^{12}\text{C}$ from the modern $^{14}\text{C}/^{12}\text{C}$ value measured by the NIST standard corrected for ^{13}C isotopic fractionation to the reference value of $\delta^{13}\text{C} = -25\%$.

3-8. Strontium isotope ratio ($^{87}\text{Sr}/^{86}\text{Sr}$)

Strontium isotopic analyses were carried out on four samples including two aragonite samples and two calcite samples.

To remove staining material, aragonite and calcite samples were immersed into diluted hydrochloric acid (~10% solution), since aragonite and calcite samples were identified and separated from the mixture by using Meigen's solution. After

measurement of sample weight, each sample was put into Teflon beaker and then 6N hydrochloric acid infused into this beaker. This beaker capped by Teflon watch glass was heated on a hot plate and waiting for vaporization of hydrochloric acid. The condition of solution was gently changed from low viscosity as water to high viscosity as gel with vaporization. Gel material was dissolved with 3ml of distilled 2.4N hydrochloric acid. This solution was centrifuged and un-dissolved impurity was separated from the solution.

This solution infused to cation-exchange resin of AG-50W-X8 and then dissolve strontium was concentrated in cation-exchange resin. For recovery strontium from cation-exchange resin, 52ml of hydrochloric acid was infused again. The amount of re-infuse hydrochloric acid (52ml) was different in each cation shown in Figure 5. Figure 5 shows a relationship between re-infuse amount and the cation sequence dissolved in hydrochloric acid. Recovered hydrochloric acid including strontium was completely evaporated on a hot plate and solid material remained in the beaker. This material was dissolved with nitric acid and this solution was evaporated by hot plate. Remaining solid material in beaker, one drop of water was infused to this beaker and remaining material was dissolved into the water and then this water was put on a filament for mass spectrometric measurement. Sr isotopic compositions of calcite and aragonite were measured with a VG Sector 54-30 at Nagoya University (Asahara, 1999). Measurements of the strontium isotopic ratio of the NIST 987 standard during the analyses of the carbonate minerals averaged 0.710239 with two standard deviations of 0.000012.

4. Results

4-1. Mineralogy of the Conical Seamount chimney

The grain shape was the structure of needle, prism, platy and irregular (Figure 6) observed from the microscope. All grain, except for irregular grain, shown the white to translucent in color and irregular grain had pale yellow in color. Detail observation was carried out by using SEM (Figure 7). The grain bearing irregular outer shape did not show a clear cleavage and this grain shape was characterized by the conchoidal fracture typically observed in obsidian (Figure 7-B) and this structure suggests that this grain would be an amorphous phase. Other grains different from the irregular were well-crystallized and their outer shapes were kept on the euhedral shape. The needle and prism shapes were dominantly observed in the well-crystallized grains and a relative amount of the plate grain was small compared with the needle and prism grains. Well-crystallized grains were mostly formed the cluster composed of the same grain type and a solely distribution of a single grain shown in SEM images (Figure 7) was not observed in the chimney sample. Each individual grain size was about 500 μ m in maximum.

Based on the bulk measurement by XRD, it was concluded that the chimney was composed of only aragonite and calcite in the carbonate phases (Figure 8-A). After collecting of each type of grains, needle, prism and plate grains (Figure 7) showed aragonite peaks (Figure 8-B) with small calcite peak. Irregular shape grains did not show any sharp peak with a broad peaks at $2\theta \approx 26^\circ$, thus this type of grains was not carbonate and amorphous silica grains. Relative abundance of calcite is much smaller

than that of aragonite and its distribution was ubiquitous in this chimney. These results showed that it is difficult to completely identify aragonite and calcite based on only grain shapes. The application of staining method to separate the minerals from the mixture of calcite and aragonite was attempted.

4-2. Mineral identification

I attempted to separate calcite and aragonite from the mixture by heavy liquid of SPT. The used sample was the fragment of chimney and its grain size was sieved ranging from 125 μ m to 250 μ m. The sample of several milligrams including each mineral phase was immersed in the SPT solution adjusted to approximately 2.9 in its specific gravity at room temperature. In a few minutes, sample grains were separated in two groups, a floating grains and a sinking grains in the SPT solution. The mineral phase in each group grain was determined by XRD, and a floating and a sinking grains were composed of calcite and aragonite, respectively. These results support the efficiency of calcite and aragonite separation using the SPT solution. After mineral separation using SPT, separated mineral grain needs to carefully wash out SPT solution adhering to grains because SPT solution adjusted to high specific gravity has high viscosity.

I compared to apply Meigen's solution to metamorphic aragonite-calcite marble which was collected from the Word Creek, Cazadero, CA. This sample is a white recrystalline marble composed of mainly aragonite which was transformed during the Franciscan metamorphism of high pressure - low temperature type. This sample was

already isotopically studied using Feigl's solution by Ando (1992). Calcite can only be observed in and around the fractures. The Franciscan marble was crushed into fine grains less than 1mm in size, and then carbonates were stained by Meigen's solution. The staining condition was the same as mentioned above (§ 3-2): the staining temperature was 70°C and the staining time was 15minutes. Aragonite was stained in pale purple and the intensity of the staining color is fairly pale rather than that of the carbonate chimney. We tried to increase the treatment temperature up to 80°C, and to prolong the duration time but the staining intensity of aragonite remained nochanged. This result suggests that Meigen's solution shows less stain when applied to re-crystallized aragonite. Thus, Meigen's solution may be an advance in staining euhedral aragonite such as carbonate chimney. I attempted aragonite identification to chimney sample by Feigl's solution. The deeply stained surface of aragonite was covered by an oxidized silver-manganese complexes, while calcite was slightly stained pale brown in color. When our chimney grains were immersed in Feigl's solution, fine-grained and white color precipitation was observed. This precipitation was adhered to the surface of carbonate grains and it makes small particles amalgamating around grains. It is estimated to be silver chloride since dechlorinate treatment was not processed on our carbonate sample. This comparison of two staining solution suggested that Meigen's solution agree with the identification of aragonite and calcite compared with Feigl's solution in this sample. In comparison with staining and heavy liquid concerning the facility of mineral identification and separation, the usage of staining solution is more fitting to chimney sample in this study.

Carbonate chimney at the Conical seamount, including three types of grains were experimented with Meigen's solution. After the treatment with Meigen's solution, aragonite was completely identified from the mixture (Figure 9). The non-stained grains with Meigen's solution were composed of calcite (Figure 10-A) and irregular shape grain. Calcite was easily identified and collected from the mixture of both minerals, since the grain color and shape is quite different from the amorphous phase. The grain shape of calcite was long prism type. Whereas the stained grains in purple was composed of aragonite (Figure 10-B) and its grain type showed needle and long prism. Figure 11 shows the thin section stained by Meigen's solution and aragonite bearing yellow in color occurs as a block, which is a dominant mineral phase compared with calcite, whereas calcite bearing white in color occurs as a vein filling in the gaps of the aragonite blocks.

4-3. Relative abundance of calcite and aragonite

The results of XRD measurement of the carbonate fragment show that the mineral composition of the carbonate chimney was calcite and aragonite. The relative abundance of calcite and aragonite in the chimney was possible to estimate through an accurate XRD analysis using calibrated mixtures of calcite and aragonite by known standards, and all raw data are listed in Table 1. The relationship between peak intensity ratio of aragonite and aragonite weight percentage of sample is shown in Figure 12. Peak intensity ratio of aragonite show increment exponentially with aragonite weight ratio of sample. A regression curve calculated from these plots shows good

correlation exponentially ($R^2 = 0.945$). The relative abundance of calcite and aragonite in the chimney was estimated to be 31.6% and 68.4%, respectively by using the regression curve shown in Figure 12. The composition ratio of calcite and aragonite estimated by modal accounts using stained thin sections by NIH image 1.62f, which was image processing and analyses software (§ 3-5). The relative abundance of calcite and aragonite using NIH image was 0.28 and 0.72, respectively. The relative abundance estimation from the thin section observation and the XRD measurements indicated aragonite as a dominant mineral phase and calcite as only composed of about ~30% in the chimney.

4-4. Stable isotope measurements ($\delta^{13}\text{C}$ & $\delta^{18}\text{O}$)

To clarify the origin and formation processes of the carbonate chimney, calcite and aragonite were identified using the staining method. Separated by hand picking calcite and aragonite were analyzed for their carbon and oxygen stable isotope signatures. Figure 13 shows the cross section of the chimney marked with sample locations. The isotopic results are listed in Table 2. $\delta^{13}\text{C}$ values are plotted in narrow range between -0.48‰ and -2.12‰, whereas $\delta^{18}\text{O}$ values are plotted in wide range from +4.20‰ to +6.71‰ (Figure 14). These isotopic ranges are similar to those in previous studies (Figure 15, Haggerty, 1991).

The samples for bulk carbon and oxygen isotopic determination were collected from the loci shown in Figure 13 with A-2 to A-5. The samples indicated by #-1 to #-4 were analyzed for calcite and aragonite single phases separated by hand picking helped

by Meigen's staining. $\delta^{18}\text{O}$ values of the separated calcite and aragonite samples (#-1 ~ #-5) showed that calcite in each sample was enriched in ^{18}O as compared with those of aragonite (Figure 16). The oxygen isotopic results shown in Figure 16 indicate the variation of $\delta^{18}\text{O}$ from +2.5‰ to +6.7‰. A trend of increasing the $\delta^{18}\text{O}$ value toward the inside of the chimney was recognizable. As shown Figure 16, a systematic variation in separated samples was evidently observed in comparison with the results of bulk samples (Kato et al., 2003). These results are firstly revealed by isotopic analyses based on mineral separation. Precipitation temperature would be calculated from $\delta^{18}\text{O}$ values of aragonite and calcite, assuming an isotopic equilibrium between carbonate and water. As shown Figure 16, two horizontal lines show the estimated isotopic value of calcite and aragonite in equilibrium with seawater at the temperature of 1.5°C which observed during the "Shinkai 6500" dive #179. Calculated values of calcite and aragonite show 3.11‰ and 3.71‰, respectively, using the oxygen isotopic fractionation by O'Neil et al. (1969) for calcite and seawater and Tarutani et al. (1969) for aragonite correction. Larger $\delta^{18}\text{O}$ values than the equilibrium value shown in Figure 16 are likely to understand the presence of deep-seated another fluid which $\delta^{18}\text{O}$ value is larger than that of seawater. A general trend of enrichment of ^{18}O in both carbonates toward the inside of the chimney strongly supports the presence of the seepage expanding toward outside the chimney, although we could not observe the conduit structure in this chimney.

4-5. Radiocarbon activity ($\Delta^{14}\text{C}$)

Seven batches of the machine time were provided by the MALT (Micro Analysis

Laboratory, Tandem accelerator) of AMS at the University of Tokyo radiocarbon measurement during 2000 September ~ 2002 October. Figure 17 shows the value of $^{14}\text{C}/^{12}\text{C}$ for the NIST standard sample, SRM-4990C, measured by AMS. The variation of $^{14}\text{C}/^{12}\text{C}$ were almost plotted in range in 2σ . Radiocarbon activities of calcite and aragonite in this work were carried out in September 2000 and December 2000. Reproducibility of standard sample during the batch measurement time, about 10minutes ranged from 0.77% to 1.42%. Reproducibility of standard sample during September in 2000 to October in 2002 ranged from 0.65‰ to 1.42‰. This value suggests that machine and prepared standard sample condition was enough to measure radiocarbon activity.

Table 3 shows the bulk ^{14}C activity of the carbonate chimney by liquid scintillation method (LSC) and those of aragonite and calcite each carbonate mineral value (by AMS). The AMS ^{14}C measurement of calcite and aragonite is the first time measurement of carbonate chimneys at Mariana Forearc. The ^{14}C activity of the chimney measured by LSC (-875.0‰) and AMS (ave. -888.7‰) shows considerable depletion in ^{14}C compared with deep-seawater, which had an activity of about -240‰ (Östlund and Stuiver, 1980). $\Delta^{14}\text{C}$ value shows the relative radiocarbon activity compared with standard sample of which radiocarbon activity correspond to atmosphere in 1950 A.D. When $\Delta^{14}\text{C}$ shows 0‰, radiocarbon activity of sample is equal to standard sample, whereas negative value of $\Delta^{14}\text{C}$ means depletion of ^{14}C of sample and radiocarbon-free sample shows -1000‰.

4-6. Strontium isotope measurements ($^{87}\text{Sr}/^{86}\text{Sr}$)

Two pairs of calcite and aragonite collected from the rim and core parts of the carbonate chimney were measured to confirm Sr isotopic value. The results of the Sr isotopic measurements in each mineral and the related Sr isotopic data in this study are listed in Table 4, and Sr isotopic values showed remarkable differences in each mineral.

Strontium is an alkaline earth metal and its ionic radius shows 1.13Å which is possible to be interpolated into a carbonate mineral structure. The concentration of strontium in aragonite is higher than that of calcite, and approximately equilibrium concentration of aragonite and calcite is 1% and 1000ppm, respectively (Veizer, 1983). The large ionic radius in alkaline earth metals compared with calcium is selectively contained in aragonite rather than calcite because its crystal lattice form has a capability to accommodate these metals. ^{87}Sr is a radiogenic nuclide and stable isotope formed from β -decay of ^{87}Rb of which half life is 49.9 billion years. The variable factor of strontium isotopic ratio in seawater is recognized to be two primary source: continental crust and upper mantle, although the strontium isotopic composition of seawater is resulted from the mixing of various source materials. Continental crust is enriched in Rb which is an incompatible element and largely concentrated in silicate rocks. Continental crust supplies dissolved strontium originated from ^{87}Rb to the oceans through the chemical weathering. The upper mantle sources supply strontium originated from ^{87}Rb to the ocean through the hydrothermal activity at mid-ocean ridges and submarine weathering of oceanic basalts. Strontium isotopic ratio of seawater shows the same value in everywhere through the world ocean (Elderfield, 1986), and the

reason for a constant values is ascribed to a long oceanic residence time of strontium. In general, the scale of oceanic global circulation of sea water is estimated to be approximately two thousand years, on the contrary, strontium residence time is estimated to be a approximately four million years (Elderfield, 1986) and the scale of residence time is three order long. This fact indicates that a dissolved strontium in seawater is sufficiently mixed homogeneously taking a long time and also isotopic value of seawater shows the constant value everywhere. Table 5 shows the strontium isotopic values of carbonate and seawater in the present marine environment and its values of seawater and carbonates are corresponded with 0.7092, up to four decimal places (Elderfield, 1986). The variation of strontium isotopic ratio in seawater through a Phanerozoic was reported by Burke et al. (1982) and this variation curve was called "Burke Curve" (Figure 18). This curve was made from the measurements of 786 samples of marine origin such as fossil of foraminifera, nanofossil from DSDP cores, limestone, dolostone, carbonate, and conodonts. Burke curve has a variation in range between about 0.7092 and 0.7068, and this range is corresponded with the intermediate value between the average isotopic value of continental (~ 0.716) and submarine basalts (~ 0.703). Although the reason for this variation has not clearly demonstrated, this variation would be linked to continental growth event (Elderfield, 1986).

5. Discussion

5-1. Carbonate chimney at the Conical seamount, Mariana forearc

5-1-1. Oxygen isotope

Isotope is a good tracer tool to estimate the origin of carbonate chimney and its formation processes. An equilibrium isotopic fractionation at 25°C between calcite and aragonite shows 1.8‰ enrichment in ^{13}C for aragonite (Rubinson and Clayton, 1969), and, oxygen isotopic fractionation at 25°C in each mineral shows 0.6‰ enrichment in ^{18}O for aragonite (Tarutani et al., 1969). Table 7 shows the carbon and oxygen isotopic fractionation between calcite and aragonite in this study, and the fractionation does not show a constant value. Assuming that calcite and aragonite were precipitated from a fluid at a constant temperature, the isotopic fractionation between calcite and aragonite would show a constant value. These results were ascribed to the presence of a different fluid source and different stage for each mineral precipitation. This suggestion was supported by the results of the calculation of precipitation temperature using the oxygen isotopic values as follows.

The calculated precipitation temperatures for this study gave a range from 3.7°C to -9.7°C, assuming that carbonate precipitation occurred during an equilibrium with the seawater ($\delta^{18}\text{O} = 0\text{‰}$, SMOW). Equilibrium fractionation factors were experimentally determined for the calcite- H_2O system (O'Neil et al., 1969), and for an aragonite with additional correction between calcite and aragonite (Tarutani et al., 1969). According to the Dive #179 log by "Shinkai 6500", the ambient seawater temperature of the carbonate chimney was observed to be a constant at 1.5°C, when the submersible was resting on the Conical Seamount at a depth of 3,200m. Most of the calculated temperature was below 0°C (Table 8) and these values were considerably lower than the seawater temperature observed. The temperature estimate suggests that the oxygen isotopic value of

carbonate were not in equilibrium with the seawater and the oxygen isotopic composition of fluid related with carbonate precipitation was different from the seawater, probably from venting fluids.

On the contrary, the oxygen isotopic value of venting fluid can be calculated, assuming that the precipitation occurred at an ambient seawater temperature of 1.5°C. As shown in Table 7, the $\delta^{18}\text{O}$ values of the venting fluids are estimated to range from -0.59 to +2.85‰ (SMOW). These results are consistent with the $\delta^{18}\text{O}$ values of dehydrating water (+3‰ ~ +6.5‰) resulted from alteration of subducted oceanic crust at 400°C (Sakai et al., 1990). Moreover, these oxygen isotopic values of aragonites increased towards the core from -0.59‰ to +2.04‰ for the sample #-1 to #-4, respectively as shown in Table 8. $\delta^{18}\text{O}$ values of coexisting calcites showed also the same trend. The oxygen isotopic value of the rim part of the chimney was close to 0‰, which means the oxygen isotopic equilibrium was maintained during carbonate precipitation. Oxygen isotope values strongly suggest the existence of another fluid derived from serpentinization beneath the Conical Seamount.

5-1-2. Radiocarbon activity

The radiocarbon activity ($\Delta^{14}\text{C}$) was considerably lower than that of the ambient seawater where a $\Delta^{14}\text{C}$ value of Pacific deep-sea is about -240‰, corresponds to the age about 2,000yr.B.P. reported in GEOSECS (Östlund and Stuiver, 1980). If the chimney was directly formed from such deep seawater, the radiocarbon activity of the chimney should be similar to the value of the deep seawater. On the contrary, the radiocarbon

activity in this study is depleted considerably in ^{14}C in each mineral compared with radiocarbon activity of seawater. The low radiocarbon activity of carbonate chimney including both data of LSC and AMS suggests that the simple mixing of the ambient seawater and venting fluid depleted in ^{14}C can be plausible for the precipitation of the coexisting calcite and aragonite. The carbonate deposits precipitated in other cold seep in the present are shown extremely old radiocarbon age as $\sim 12\text{ky. B.P.}$ of botryoidal aragonite in Bahama (Grammer et al., 1993), 33ky. B.P. of dolomite chimney at Otago in New Zealand (Orpin, 1997), these old ages are clearly contributed by the dead carbon source which is different from seawater. Therefore, low radiocarbon activity in this study is also affected by the dead carbon source, and it may be ascribed to a deep-seated fluid formed during serpentinization process beneath the Conical Seamount. Radiocarbon activity for dead carbon is described as -1000‰ in $\Delta^{14}\text{C}$ scale, radiocarbon activity of calcite and aragonite would be -1000‰ , if each mineral precipitated directly from the dead carbon source. Calcite and aragonite are resulted from the mixing of seawater and the fluid composed of dead carbon, since the radiocarbon activities of calcite and aragonite are distributed between the seawater (-240‰) and the dead carbon value (-1000‰). Assuming that two endmembers; one is the seawater to be $\Delta^{14}\text{C} = -240\text{‰}$ and to be 2mmol/l for carbonic acid reported from Haggerty (1991), and the another is the fluid related to serpentinization to be $\Delta^{14}\text{C} = -1000\text{‰}$ and to be 9.3mmol/l for concentration of carbonic acid. Concentration of carbonic acid was estimated from the result of interstitial water of drill core, site 780 (Mottl, 1992) and detail description was written in later section (§ 5-1-4). Reaction formula of serpentinization was

expressed as;

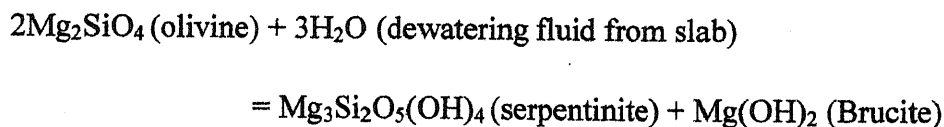


Figure 19 shows the calculation results of two fluids mixing ratio during calcite and aragonite precipitation, and aragonite gives a mixing ratio of 40% ~ 46% for venting fluid composed of dead carbon and 54% ~ 60% for seawater, whereas calcite gives the value of 83% ~ 90% for venting fluid and 10% ~ 17% for seawater.

5-1-3. $^{87}\text{Sr}/^{86}\text{Sr}$ ratio

Assuming that calcite and aragonite are precipitated from the same fluid having a constant strontium isotopic ratio, strontium isotopic values of calcite and aragonite should show the same values. $^{87}\text{Sr}/^{86}\text{Sr}$ ratio of aragonite in this study are very close to seawater (Table 3, 4), therefore it is clear that origin of the strontium is considered to be seawater during aragonite precipitation. Bonatti (1980) reported the strontium isotopic ratio of aragonite precipitated in the serpentinized peridotite collected from the Vema Fracture Zone in the water depth ranged from 3,850m to 4,900m (10°56.2'N, 43°36.0'W) was 0.7097 and summarized that this strontium was originated from seawater in combination with the results of carbon and oxygen isotopic results.

On the other hand, strontium isotopic values of calcite show completely different values in comparison with aragonite values (Table 3). Strontium isotopic value of calcite suggest the presence of the different strontium source for calcite precipitation. The strontium isotopic values of calcite are similar to that of the interstitial water

($^{87}\text{Sr}/^{86}\text{Sr} = 0.70624 \pm 0.000012$) at 129.9 meters below surface (mbsf) from the site 780C, ODP leg125 (Haggerty and Chaudhuri, 1992), and detail map describing boring sites around the Conical Seamount during ODP leg 125 are shown in Figure 20.

Two strontium isotopic analyses of interstitial water recovered from 3.9 mbsf and 129.9 mbsf of the site 780c were carried out by Haggerty and Chaudhuri (1992) and their strontium isotopic ratios were 0.70912 and 0.70624, respectively. These results suggest a simple mixing of two strontium source, one is seawater ($^{87}\text{Sr}/^{86}\text{Sr} = 0.709211 \pm 0.000037$, Elderfield, 1986) and the other is venting fluid ($^{87}\text{Sr}/^{86}\text{Sr} = \text{unknown}$, at least below 0.7062). Strontium isotopic composition in venting fluid is linearly added by seawater component with decreasing sub-bottom depth. Although I can not embody the upwelling mechanism without mixing of seawater component during calcite precipitation, strontium isotopic ratio of calcite has clearly suggested the presence of deep-seated fluid source having a low strontium isotopic ratio reported by Haggerty and Chaudhuri (1992).

Mixing ratios of seawater and venting fluid are estimated by using strontium isotopic ratio in each mineral. Two-endmembers are assumed for calculation, one is the seawater to be $^{87}\text{Sr}/^{86}\text{Sr} = 0.70921$ and to be $91.3\mu\text{mol/l}$ for the concentration of an average seawater, and the another is the fluid related to serpentinization to be $^{87}\text{Sr}/^{86}\text{Sr} = 0.70525$, which value is the lowest strontium isotopic value in interstitial water collected from Conical seamount during ODP leg 125, site 779A, 105-110mbsf (Haggerty and Chaudhuri, 1992) and to be $10\mu\text{mol/l}$ for concentration estimated value from Mottl (1992). Figure 21 shows the calculation results of two fluids mixing ratio during calcite and aragonite precipitation, and aragonite gives a mixing ratio of 8% ~ 18% of the

venting fluid and 82% ~ 93% for the seawater, whereas calcite gives the value of 93.6% ~ 94.1% for the venting fluid and 5.9% ~ 6.4% for the seawater.

Mixing ratios during calcite precipitation showed a good agreement with radiocarbon activity and strontium isotopic ratio. On the contrary, mixing ratios of aragonite was not in agreement with the results between radiocarbon activity and strontium isotopic ratio, and the radiocarbon data show significantly low ratios with regards to the strontium isotopic ratios. The radiocarbon data of aragonite strongly suggests another phenomenon different from simple mixing of two fluids. Strontium isotopic values of calcite suggest the change of strontium isotopic composition in the fluid before and after aragonite precipitation. As mentioned in the earlier sentence, an approximate equilibrium concentration of strontium in aragonite and calcite is about 1% and 1000ppm, respectively (Veizer, 1983). At the aragonite precipitation, seawater origin of strontium is selectively coprecipitated into aragonite because relative abundance of seawater strontium is higher (91.3 μ mol/l) than that of venting fluid (~10 μ mol/l) and then the strontium isotopic composition of aragonite was shifted to the strontium isotopic composition of seawater. The results of strontium isotopic ratio show a simple mixing of the seawater and the venting fluid at calcite precipitation. On the other hand, the strontium isotopes in aragonite reflects a concentration process of seawater strontium at aragonite precipitation and it is strongly ascribed to the geochemical and mineralogical differentiation of strontium.

5-1-4. Precipitation of aragonite and calcite

The formation of the carbonate phase of calcite and aragonite is largely controlled by the dissolved metal concentration in the solution. Kitano (1962) reported that Mg^{2+} concentration is the largest factor of aragonite precipitation by their experimental results and Figure 22 shows an increase in the relative aragonite precipitation ratio with Mg^{2+} concentration in the solution. Aragonite is preferentially precipitated at higher than 400ppm for Mg^{2+} concentration in the solution and calcite precipitation appears in a low concentration (Kitano, 1962).

Geochemical study of pore water collected from a drilling core during ODP leg125, and chemical composition of the pore water was characterized by a low Mg^{2+} concentration showing 0.21ppm (Figure 23, Mottl, 1992). Whereas magnesium concentration in seawater is about 1290ppm. Magnesium concentration in the mixing fluid between the seawater and the venting fluid is similar to the seawater values, and this fluid chemistry will favor to aragonite precipitation rather than calcite.

Carbonate precipitation including aragonite and calcite is triggered by the venting fluid having highly alkalinity. Concentration of carbonic acid in the venting fluid was calculated using an alkalinity (62.6meq/l) which was estimated as carbonate alkalinity of the venting fluid reported by Mottl (1992). Since the concentration of B in an interstitial water was larger than that of seawater (Figure 23), an alkalinity of the venting fluid was controlled by B and carbonic acid. The chemical form of B in the solution was $B(OH)_3$ and $B(OH)_4^-$. Therefore, total alkalinity of the venting fluid was expressed as follows;

$$\text{Alk. total} = B(OH)_3 + B(OH)_4^- + H_2CO_3 + HCO_3^- + CO_3^{2-}$$

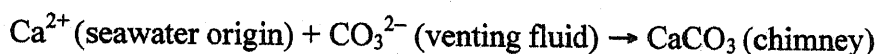
To determine chemical form of B in the venting fluid, electrolytic dissociation constant (pK_B) was calculated using the following equation introduced by Kitano (1990);

$$K_B = ([B(OH)_4^-] [H^+]) / ([B(OH)_3])$$

$$pK_B = -\log K_B = 2291.9/T + 0.01756 T - 3.385 - 0.32051 Cl^{(1/3)}$$

where T: absolute temperature, 274.5K of observed seawater temperature by "Shinkai 6500", Cl: chlorinity, 19.5‰ (Mottl, 1992), and pK_B was calculated to $10^{-9.1}$. Figure 24 shows the relationship between pH and carbonic acid species (Morse and Mackenzie, 1990). The venting fluid of pH was 12.6 (Mottl, 1992) and this value probably controlled by serpentinization formation process. The chemical species in the venting fluid was composed of $B(OH)_4^-$ and CO_3^{2-} and these species controlled alkalinity of the venting fluid. Alkalinity of B in the venting fluid was calculated to 4.1meq/l using B concentration (4mmol/l) of interstitial water (Mottl, 1992). According to the chemical compositions of the interstitial water at the site 780C of ODP drilling core, the total anions and cations are listed in Table 6. Main anions measured were ammonia, sulfate, borate, and chlorine. Main cations measured were sodium, potassium, magnesium, calcium, lithium, strontium, barium, manganese, and rubidium. As noted in previous section, the amount of the carbonic ions was not directly determined. The difference between total cations and anions are still exist in the interstitial water at the Conical Seamount. It will be possible that the excess anions probably due to the hydroxide ions originated from brucite and the carbonic ions interstitial water. The amount of the hydroxide ions was estimated from the pH of the interstitial water and its concentration was 0.040mmol/l (40meq/l). The amount of the excess anion probably carbonic ions

was calculated to be about 9.3mmol/l(18.5meq/l). Therefore, alkalinity of CO_3^{2-} was 18.5meq/l in the venting fluid, which value was calculated from total alkalinity (62.6meq/l) minus B (4.1meq/l) and hydroxide alkalinity (40meq/l). Since concentration CO_3^{2-} (mmol/l) corresponds to half value to alkalinity, concentration of carbonic acid of the venting fluid was approximately 9.3mmol/l and this value was larger than that of seawater ($\sim 2\text{mmol/l}$). Therefore, formation of carbonate chimney resulted from mixing of the venting fluid containing high carbonic acid and seawater providing Ca^{2+} , as following;



and carbonate mineral phase is controlled by the magnesium concentration in the fluid.

Mineral precipitation order is also estimated that aragonite is previously precipitated and calcite is subsequently precipitated. This assumption is supported by the thin section observation. Figure 11 shows the distribution of aragonite and calcite in thin section, and blocky aragonite is dominantly occupied in the thin section, whereas calcite occurs in filling gaps and small fractures in the aragonite block. This figure clearly suggests that aragonite was precipitated in an initial stage of carbonate precipitation and then calcite was followed in secondary. In an initial stage of chimney formation, aragonite is selectively and rapidly precipitated from the mixing fluid by the decrease of partial pressure of carbon dioxide and chemical control of high magnesium concentration. These aragonite act as barrier with time and the mixing of seawater and venting is difficult in the inside part of chimney. In later stage, calcite is precipitated in the small spaces of aragonite precipitations under a low contribution of seawater.

5-1-5. Origin of carbon

It is difficult to estimate carbon source of the venting fluid directly, since the data set of $\delta^{13}\text{C}$ of dissolved inorganic carbon (DIC) in the venting fluid is absent through previous studies related with carbonate chimney of Conical Seamount. Carbon isotopic results of calcite and aragonite forming the chimney range from -0.48‰ to -2.24‰ and these values are similar to the dissolved inorganic carbon in seawater, slightly depleted in ^{13}C . Carbon isotopic value of aragonite in deep seafloor shows a range from $+1.12\text{‰}$ to -1.7‰ (Bonatti et al., 1980; Früh-Green et al., 1996) and carbon source is estimated in DIC ($\delta^{13}\text{C} \approx 0\text{‰}$). Carbon source of aragonite of chimney is ascribed to DIC, since aragonite was precipitated from the highly mixing ($\sim 90\%$) of seawater.

Since calcite precipitation was resulted from the mixing of seawater ($\sim 50\%$) and venting fluid ($\sim 50\%$), the origin of the carbon from the venting fluid is mostly contributed to calcite precipitation compared with aragonite precipitation. A supposed carbon source of the venting fluid may have hydrocarbon, subducted organic material, subducted carbonates from microfossils such as foraminifera, and subducted carbonate resulted from water-rock interaction near sub-bottom surface. Hydrocarbon was observed in the pore water in the drill core (Mottl, 1992) and water sample collected from the inside part of chimney (Haggerty, 1991). Haggerty (1991) ascribed to hydrocarbon in pore water and venting fluid for carbon source of chimney. Assuming that carbon source of calcite is hydrocarbon, carbon isotopic value of carbon dioxide oxidized from hydrocarbon would show below -30‰ since carbon isotopic composition

is extremely depleted in ^{13}C either biogenic or thermogenic hydrocarbon and this relation is represented methane index (Figure 25). This diagram shows the relationship between carbon number of hydrocarbon and its carbon isotopic values at site 808 of ODP leg131, Nankai Trough. Carbonate deposits originated from thermogenic and biogenic methane were observed in accretionary prism (i.e., Nankaitrough; Sakai et al., 1992, Oregon off; Kulm et al., 1992) and offshore oil field (i.e., North Sea; Hovland et al., 1987) and its isotopic values shown in Figure 26. It is clear that carbonates related to hydrocarbon show extremely negative carbon isotopic value. If calcite of chimney is precipitated from carbon oxidized from hydrocarbon, its carbon isotopic value should show negative values as same as above mentioned carbonates. Therefore hydrocarbon is excepted from the carbon source of calcite.

Carbon isotopic value of organic material in the oceanic sediment shows range from -20‰ to -30‰ (Sakai and Matsuhisa, 1996). The isotopic value of carbon dioxide also shows range from -20‰ to -30‰ which is resulted from the oxidation of organic material and shows a similar value to original isotopic composition of the carbon source, therefore organic material is also excepted from the carbon source of calcite.

Carbon isotopic value of carbonates in foraminifera are similar to carbon isotopic value of chimney. Although carbonates of foraminifera in sediment may be a reasonable carbon source for chimney, considering water depth of the Pacific Ocean, carbonates of foraminifera are also excepted from the carbon source of calcite. An average water depth of Pacific Ocean (4,282m, Chronological Scientific Tables, 1996) and Mariana Trench is deeper than that calcium compensation depth (about 4,000, Moore,

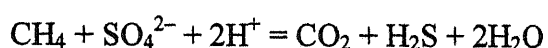
1989). This relation suggests that most of microfossils in the sediment are dissolved in seawater before subduction at trench, thus, isotopic component of foraminifera are not contained to the venting fluid, although the summit of the Conical Seamount is shallow (3,200m) to calcium compensation depth.

Carbon isotopic value of carbonate resulted from water-rock interaction near sub-bottom surface shows the similar value to DIC (Bonatti et al., 1980; Früh-Green et al., 1996) and to carbonate chimney of Conical Seamount (Figure 26). Bonattie et al. (1980) suggested aragonite precipitate during reaction between ultramafic rocks and circulating seawater and carbon source of these aragonite were originally seawater. Assuming that a large amount of this carbonate subducted at trench system, a subducted carbonate phase would be dissolved to fluid which was accompanied with subducting crust as carbon dioxide with increase of pressure and temperature. Although it is still unknown for its distribution scale in the seafloor, this carbonate would be the most reasonable carbon source of calcite in the several supposable carbon sources. The carbon isotopic composition of the venting fluid would be made from the mixing of several supported carbon sources such as above mentioned.

5-2. Carbonate cement related to an old cold seepage

Carbonate cement characterized by highly depleted ^{13}C was observed in the present marine and on the land outcrops along a convergent margin. The grain size of cementation was small as several micro millimeters and aragonite, calcite and dolomite were coexisted in the same cementation. Generally, these cementation was precipitated

in the matrix of sediment composed of fine-grained sand or muddy sand, it is difficult to separate in each mineral from the multi-mineral carbonate phase. The carbon source of these cementations was originated from carbon dioxide induced by the oxidation of methane with microbial activity on sulfate-reduction in the sediment and reaction type was as follow;



Carbon isotopic composition of these cementations are characterized by highly negative values and the range of $\delta^{13}\text{C}$ value shows from -40‰ to -60‰ (i.e. Shibazaki and Majima, 1997). Although the isotopic studies concerning these cementations were carried out and have suggested the mixing model between seawater and another fluid for formation of cementation, the mixing ratio of two fluids and chemical evolution has not been discussed from the isotopic analyses because previous studies did not analyze mineral separates from the cementations. In here, I will introduce the preliminary result concerning the isotopic analyses of carbonate cementation and the problem for mineral separation of carbonate cementation in fine-grained size, although this study is not completely finished.

5-2-1. Konandai, Kanagawa

Tate and Majima (1998) reported an outcrop including the chemosynthesis fossil community and carbonate cementation in the Koshiba Formation which is an outer shelf facies of the lower Pleistocene, Miura Peninsula, Kanagawa Prefecture, central Japan (Figure 27). The assemblage of the fossil bivalve consists mainly of large size, attaining

10cm in maximum diameter, *Lucinoma* sp. and *Conchocele* in association with sparsely or massively developed carbonate cementations (Tate and Majima, 1998). Four boring cores were recovered from the outcrop of this cold seep assemblages in order to clarify the distribution of the chemosynthetic bivalve assemblages and the origin of carbon in cementation. Total length of cores was at about 100m. Figure 28 shows detail topographic map of boring site and the position of each boring. The core A is 20m in length and was bored to parallel to the bedding plane from a point where bivalve fossils are mostly concentrated in the outcrop. The core B (25m in length), core C (40m) and core D (15m) were bored vertical direction to the bedding plane: cores B and D from the foot of the lower outcrop and core C from the ridge just above the fossil and cement outcrop (Figure 29). I will introduce the preliminary results on mineral composition and isotopic analyses of cementation in the core D. More detail description concerning the fossil assemblages and geological setting in this area were reported by Kitazaki and Majima (2002).

The total length of core D was 15m and its lithofacies was gently changed from mudstone to sandstone toward an upper part of this core. Figure 30 shows the picture and sketch of core D. The part of cement was described in the dotted area and the sampling positions for determination of carbonate mineral phase by XRD and analyses of carbon and oxygen isotopes were expressed in small circles in red color. The mineral composition of cements were characterized by two mineral assemblages which one assemblage was calcite and aragonite, another was dolomite and calcite. The former assemblage was distributed in dominantly in the upper part range from 0m to 8m,

whereas the latter assemblage was observed in the lower part from below 8m (Figure 30). Preliminary results of carbon and oxygen isotopic of calcite and aragonite were listed in Figure 30. Oxygen isotopic values show a small variation range from +2.71‰ to +3.22‰ (Figure 31). These oxygen isotopic results suggest that the isotopic composition of carbon source in fluid was constant through a cementation of this core. On the hand, carbon isotopic values distribute in a ranging from -58.68‰ to -44.54‰. A large variation was observed in carbon isotopic value (Figure 31). These values show the similar value to other carbonate deposits related to methane seepage area observed in the present marine environment, for example Nankai Trough (Sakai et al., 1992) and off Oregon (Kulm and Suess, 1990). Although it is difficult to explain a large isotopic variation in core D from only my data set, a possible carbon source orientation is mentionable. Paull et al. (1992) reported the relationship of highly negative $\delta^{13}\text{C}$ value corresponding to the high ΣCO_2 concentration in pore water at the Florida escarpment, where the colony of chemosynthetic organism and high concentration of CH_4 in the pore water were observed. These relationship were reflected by microbial oxidation of CH_4 in the sediment. When we considering these results and the precipitation processes will increase ΣCO_2 concentration and deplete their $\delta^{13}\text{C}$ value. Considering this report, a large $\delta^{13}\text{C}$ variation in boring core D would be arisen from the heterogeneity of ΣCO_2 concentration in pore water.

5-2-2. Shintomi town, Miyazaki

The carbonate cementation resulted from cold seepage is exposed at Shintomi

Town, Koku County, Miyazaki Prefecture and occurs in the Takanabe Formation of the Miyazaki Group which are deposited forearc basin during Pliocene. The Takanabe Formation was distributed in the coastal area of Miyazaki Prefecture (Figure 32). The Miyazaki Group overlies the pre-Miocene highly deformed Shimanto subduction complex and is overlain by the Pleistocene fluvial and marine terraces, and displays an overall N-S trend with an eastward tilting. The carbonate cementation was outcropped near the Kuge Shrine at Shintomi town. The carbonate cemented sample was dominantly composed of tuffaceous sandstone with many bivalve fossils of *Lucinoma* sp (Majima and Ikeda, submitted). Any vein structures composed of carbonates were not observed in this sample and carbonate cementation was precipitated in the matrix of tuffaceous sandstone. Carbonate mineral phase in this cement was calcite detected by using XRD. The preliminary isotopic results were listed in Table 9.

Oxygen isotopic values show a range from -4.94‰ to $+1.59\text{‰}$. This oxygen isotopic result shows relatively a wide variation compared with boring core D mentioned in the previous chapter. Carbon isotopic values show a range from -30.69‰ to -53.21‰ . These values show a similar value to other carbonate deposits related to methane seepage area. Figure 33 show the diagram of carbon and oxygen isotopic values of these samples. This figure shows the relationship between $\delta^{13}\text{C}$ and $\delta^{18}\text{O}$. The factor of negative $\delta^{18}\text{O}$ values could plausibly of the presence of fresh meteoric water during cementation, this diagram would be shown the mixing line of two end-member fluid source, one is meteoric water and another is the pore water including the carbon dioxide oxidized from methane presented in sediment.

6. Summary

In order to identify aragonite from polycarbonate samples, Meigen's and Feigl's solutions are useful for micro-scale isotopic analyses. Our preliminary results of individual mineral identified using Meigen's solution show high advantage for sample collection of an aragonite grain for their isotopic analyses. Moreover, our results suggest that the mineral identification and separation are important procedures for isotopic analyses to clarify the origin and the formation process.

Isotopic measurements of calcite and aragonite separated from a coexisting condition using the staining method revealed the mixing ratio between the seawater and the venting fluid related with serpentinization.

According to the carbonate chimney at Conical Seamount in the Mariana Forearc region, the mixing ratios calculated from $\Delta^{14}\text{C}$ and $^{87}\text{Sr}/^{86}\text{Sr}$ ratio are as follows: (I) The mixing ratio of carbon between the seawater and the venting fluid calculated from $\Delta^{14}\text{C}$ during aragonite precipitation is 60% and 40%, respectively, (II) The mixing percentages between the seawater and the venting fluid calculated from $\Delta^{14}\text{C}$ data during calcite precipitation are 10% and 90%, respectively. These results indicated the presence of different stage of calcite and aragonite precipitations in the chimney, and aragonite was precipitated prior to calcite precipitation. (III) The mixing percentages of strontium between the seawater and the venting fluid calculated from $^{87}\text{Sr}/^{86}\text{Sr}$ ratio during aragonite precipitation are 90% and 10%, respectively. (IV) The calculated mixing ratio of strontium at aragonite precipitation does not show an apparent ratio of water itself

because Sr component of seawater originated in the fluid is selectively concentrated in aragonite during its precipitation.

The mineral precipitation process can be estimated as follows: (I) seepage fluid composed of dead carbon, slightly enriched in ^{18}O relative to the seawater, and low Mg^{2+} content vents to the sea floor, (II) venting fluid starts to mix with the seawater, (III) and then aragonite precipitation starts in the initial stage of flow of the venting providing high concentration Mg^{2+} from the ambient seawater, (IV) calcite precipitation occurs in the later stage filling fractures in aragonite framework protected by aragonite deposit from seawater.

Our results indicate that the ^{14}C activity in the carbonate chimney is low because the precipitation from the seepage fluid containing dead carbon. Hence the radiocarbon age of the carbonate chimney cannot be used directly to determine its formation age. This would apply to the age determination of carbonate deposits formed from cold seepage of methane hydrate and groundwater. The same phenomenon is known for organisms living in a cold seepage (Paull et al., 1989).

According to Fryer et al. (1999), the chemical differences (especially Mg) in pore waters seeps from the deep serpentinized forearc mud volcanoes in the Mariana convergent margin. At the Conical Seamount, the presence of carbonate chimneys may indicate that decarbonation of reaction progressed at depth between 15 km and 20 km in the Mariana subduction zone (Fryer et al., 1999). Our work shows that the presence of aragonite and calcite in carbonate chimney is strongly related to the mixing process of seawater and the deep-derived fluid in the mud volcanoes associated with the serpentine

diapirs. Carbon, oxygen and strontium isotopic signatures provide a useful tool in understanding the mixing process of the two different fluids.

Staining technique would be a useful mineral identification and/or separation to carbonate cementations composed of multi-carbonate mineral phases coexisting with chemosynthesis fossils of molluscan that is originated to cold seepage and appears on land (i.e., Cavagna et al., 1999). They include a few carbonate mineral assemblages such as calcite, aragonite, and dolomite in the sediment. Multistage staining method would provide us with a complete and excellent mineral separation technique on multi carbonate rocks. These cementations give us adequate data of seepage fluid evolution in the past.

Supervised: Professor Hideki Wada

Acknowledgements

I would like to special thank Dr. K. Fujioka of JAMSTEC and Dr. N. Niitsuma of Shizuoka University for giving us useful suggestions and discussions through my doctoral course studies. I wish to thank Dr. K. Kobayashi, Dr. H. Matsuzaki, and Dr. Y. Sunohara for the AMS measurement at The University of Tokyo, Dr. H. Kitagawa and Dr. H. Takahashi for the AMS sample preparation at Nagoya University, and Dr. T. Tanaka, Dr. Y. Asahara, Dr. M. Minami, and Mr. M. Tsuboi for the Sr isotope measurement at Nagoya University. I also wish to thank Dr. A. Orpin of National Institute of Water and Atmospheric Research at New Zealand, Dr. T. Masuzawa of Nagoya University, Dr. K. Kato, Dr. M. Satish-Kumar, and Mr. S. S. Binu-Lal of Shizuoka University for discussion and correction of English grammar in this thesis, and Miss. M. Nagayama, Mr. Y. Tada, Miss. R. Tsuchiya, Miss. Mr. Y. Fujitani, M. Mochizuki, Mr. K. Mori, Mr. T. Kawai, and Mr. S. Takahashi for help during the different stages of the present study at Shizuoka University.

References

- Ando, T., (1992MS), Geochemical study of the Cazadero area in the Franciscan metamorphic belt, California. *B. Sc. Thesis, Shizuoka Univ.*, 43pp, (in Japanese with English abstract).
- Asahara, Y., (1999), $^{87}\text{Sr}/^{86}\text{Sr}$ variation in north Pacific sediments: a record of the Milankovitch cycle in the past 3 million years, *Earth and Planetary Science Letters*, **171**, 453-464.
- Berke, W. H., Denison, R. E., Hetherington, E. A., Koepnick, R. B., Nelson, H. F., and Otto, J. B., (1982), Variation of seawater $^{87}\text{Sr}/^{86}\text{Sr}$ throughout Phanerozoic time, *Geology*, **10**, 516-519.
- Berner, U., and Faber, E., (1993), Light hydrocarbons in sediments of the Nankai accretionary prism (Leg 131, Site 808), in Hill, I. A., Taira, A., Firth, J. V. et al. (eds), *Proceedings of the Ocean Drilling Program, Scientific Results*, **131**, pp.185-195.
- Bonatti, E., Lawrence, J. R., Hamlyn, P. R., and Breger, D., (1980), Aragonite from deep sea ultramafic rocks, *Geochimica et Cosmochimica Acta*, **44**, 1207-1214.
- Cavagna, S., Clari, P. and Martire, L., (1999), The role of bacteria in the formation of cold seep carbonates: geological evidence from Monferrato (Tertiary, NW Italy), *Sedimentary Geology*, **126**, 253-270.
- Chronological Scientific Tables, (1996), National Astronomical Observatory (ed.), Maruzen Co., Ltd., 1043p.
- Danhara, T., Iwano, H., Kasuya, M., Yamashita, T., and Sumii, T., (1992), The use of sodium polytungstate, a new nontoxic heavy liquid, *Chishitu News*, **455**, 31-36.
- DePaolo, D. J., and Ingram, B. L., (1985), High-resolution stratigraphy with strontium isotopes, *Science*, **227**, 938-941.
- Elderfield, H., and Geraves, M. J., (1981), Strontium isotope geochemistry of Icelandic geothermal systems and implications for seawater chemistry, *Geochimica et Cosmochimica Acta*, **45**, 513-528.
- Elderfield, H., (1986), Strontium isotope stratigraphy, *Palaeogeography, Palaeoclimatology, Palaeoecology*, **57**, 71-90.
- Friedman, I., and O'Neil, J. R., (1977), Complication of stable isotope fractionation factors of geochemical interest, in Fleisher, M. (ed.), *Data of Geochemistry, Chapter KK, United States Geological Survey. Professional Paper*, **440-KK**, 12p.

- Früh-Green, G.L., Plas, A., and Lécuyer, C., (1996), Petrologic and stable constraints on hydrothermal alternation and serpentinization of the EPR shallow mantle at Hess Deep (site 895), in Mével, c., Gills, K. M., Allan, J. F., and Meyer, P. S. et al. (eds), *Proceedings of the Ocean Drilling Program, Scientific Results*, **147**, pp.255-291.
- Fryer, P., Saboda, K. L., Jhonson, L. E., Mackay, M. E., Moore, G. F., Moore, G. F., and Stoffers, P., (1990), Conical seamount: SeaMARK II, ALVIN submersible, and seismic-reflection studies, in Fryer, P., Pearce, J. A., Stokking, L. B. et al. (eds), *Proceedings of the Ocean Drilling Program, Initial Report*, **125**, pp.69-80.
- Fryer, P., (1996), Evolution of the Mariana convergent plate margins system, *Review of Geophysics*, **34**, 89-125.
- Fryer, P., Wheat, C. G., and Mottl, M. J., (1999), Mariana blueschist mud volcanism: Implications for conditions within the subduction zone, *Geology*, **27**, 103-106.
- Fujioka, K., Wada, H., Okino, K., Debari, S., Tokuyama, H., Naganuma, T., Ogawa, Y., Fryer, P., Aoike, K., Kato, H., and Nishimura, H., (1994), Izu-Bonin transect dive program -Cross section of oceanic crust, serpentine seamount, manganese pavement-, *JAMSTEC Journal of Deep Sea Research*, **10**, 1-35 (in Japanese, with English Abstr.).
- Grammer, G. M., Ginsburg, R. N., Sware, P. K., McNeill, D. F., Jull. A. J. T., and Prezbindowski, D. R., (1993), Rapid growth rates of syndepositional marine aragonite cements in steep marginal slopedeposits, Bahamas and Belize, *Journal of Sedimentary Petrology*, **63**, 983-989.
- Haggerty, J.A., (1987), Petrology and geochemistry of Neogene sedimentary rocks from Mariana Forearc seamounts: Implications for emplacement of the seamounts, in Seamounts, islands, and atolls, edited by Keating, B., Fryer, P., and Batiza, R., *American Geophysical Union Monograph*, **43**, 175-185.
- Haggerty, J., and Cloutier, M. J., (1988), Biologic and mineralogic studies of deep-sea chimneys venting cold water from Mariana forearc seamounts. *Geol. Soc. Am. Abstracts Programs*, **20**, A199. (Abstract)
- Haggerty, J. A., (1991), Evidence from fluid seeps atop serpentine seamounts in the Mariana Forarc: Clues for emplacement of the seamounts and their relationship to forearc tectonics, *Marine Geology*, **102**, 293-309.
- Haggerty, J. A., and Chaudhuri, S., (1992), Strontium isotopic composition of the interstitial water from leg 125: Mariana and Bonin forearcs, in Fryer, P., Pearce, J.

- A., Stokking, L. B. et al. (eds), *Proceedings of the Ocean Drilling Program, Scientific Report*, **125**, pp.397-400.
- Hattori, M., Oba, T., Kanie, Y., and Akimoto, K., (1994), Authigenic carbonates collected from cold seepage area off Hatsushima Island, Sagami Bay, central Japan, *JAMSTEC Journal of Deep Sea Research*, **10**, 405-416.
- Hess, J., Bender, M. L., and Schilling, J. G., (1986), seawater $^{87}\text{Sr}/^{86}\text{Sr}$ evolution from Cretaceous to present – Applications to Paleooceanography, *Science*, **231**, 979-984.
- Holmes, A., (1921), Petrographic methods and calculations. Thomas Murby & Co., 515pp.
- Hovland, M., Talbot, M. R., Qvale, H., Olausson, S., and Aasberg, L., (1987), Methane-related carbonate cements in pockmarks of the North Sea, *Journal of Sedimentary Petrology*, **57**, 881-892.
- Hutchison, C. S., (1974), Laboratory Handbook of Petrographic Techniques. John Wiley & Sons, 690pp.
- Kato, K., Wada, H., and Fujioka, K., (2003), The application of chemical staining to separate calcite and aragonite minerals for micro-scale isotopic analyses, *Geochemical journal*.
- Kato, K., and Wada, H., (2001), calcite-aragonite mineral separation using staining method for micro-scale isotopic analyses, *Geoscience reports of Shizuoka University*, **28**, 25-31.
- Kitagawa, H., Masazawa, T., Nakamura, T., and Matsumoto, E., (1993), A batch preparation method of graphite targets with low background for AMS ^{14}C measurements, *Radiocarbon*, **35**, 295-300.
- Kitano, Y., (1962), The behavior of variation inorganic ions in the separation of calcium carbonate from a bicarbonate solution, *Bulletin of the Chemical Society of Japan*, **35**, 1973-1980.
- Kitazaki, T., and Majima, R., (submitted), A fossil cold-seep assemblage on a slope to outer shelf environment in the fore-arc basin fill, Plio-Pleistocene Kazusa Group, Pacific side of central Japan, *Paleontological Research*.
- Kobayashi, K., Matsuzaki, H., Hatori, S., Nakano, C., Yamashita, H., Makita, H., and Sunohara, Y., (2000), Multi-nuclide AMS with a middle-sized tandem accelerator of MALT, *Nuclear Instruments and Methods in Physics Research. Section B*, **172**, 75-81.

- Kulm, L. D., Suess, E., Moore, J. C., Carson, B., Lewis, B. T., Ritger, S. D., Kadoko, D. C., Thornburg, T. M., Embley, R. W., Rugh, W. D., Massoth, G. J., Langseth, M. G., Cochrane, G. R., Scamman, R. L., (1986), Oregon subduction zone: venting, fauna, and carbonates, *Science*, **231**, 561-566.
- Kulm, L.D., and Suess, E., (1990), Relationship between carbonate deposits and fluid venting, Oregon accretionary prism, *Journal of the Geophysical Research*, **95**, 8899-8915.
- Majima, R., and Ikeda, K., (submitted), A cold-seep assemblage in outer shelf facies of the fore-arc basin fill, Pliocene Takanabe Formation, Kyusyu Island, Japan, *Paleontological Research*.
- Masuzawa, T., Nakatsuka, T., and Handa, N., (1995), Geochemistry of pore waters from a bathyal *Calyptogena* community off Hatsushima Island, Sagami Bay, Japan, in Sakai, H., and Nozaki, N. (eds), *Biogeochemical Processes and Ocean Flux in the Western Pacific*, pp.407-421.
- Moore, C. H., (1989), Carbonate diagenesis and petrology, *Developments in Sedimentology*, **46**, Elsevier Science Publishers B.V., 338p.
- Morse, J. W., and Mackenzie, F. T., (1990), Geochemistry of sedimentary carbonates, *Developments in Sedimentology* **48**, 510pp.
- Mottl, M. J., (1992), Pore water from serpentinite seamounts in the Mariana and Izu-Bonin Forearcs, Leg 125: Evidence for volatiles from the subducting slab, in Fryer, P., Pearce, J. A., Stokking, L. B. et al. (eds), *Proceedings of the Ocean Drilling Program, Scientific Report*, **125**, pp.378-385.
- O'Neil, J. R., Clayton, R. N., and Mayeda, T. K., (1969), Oxygen isotope fractionation in divalent metal carbonates, *The Journal of Chemical Physics*, **51**, 5547-5558.
- Orpin, A. R., (1997), Dolomite chimney as possible evidence of coastal fluid expulsion, uppermost Otago continental slope, southern New Zealand, *Marine Geology*, **138**, 51-67.
- Östlund, H. G., and Stuiver, M., (1980), GEOSECS Pacific radiocarbon, *Radiocarbon*, **22**, 25-53.
- Palmer, M. R., and Elderfield, H., (1985), Sr isotope composition of sea water over the past 75 Myr, *Nature*, **314**, 526-528.
- Paull, C. K., Martens, C. S., Chanton, J. P., Neumann, A. C., Coston, J., Jull, A. J. T., and Toolin, L. J., (1989), Old carbon in living organisms and young CaCO₃

- cements from abyssal brine seeps, *Nature*, **342**, 166-168.
- Paull, C. K., Chanton, J. P., Neumann, A. C., Coston, J. A., and Martens, C. S., (1992), Indicators of methane-derived carbonate and chemosynthetic organic carbon deposits: Examples from the Florida escarpment, *Palaios*, **7**, 361-375.
- Robert, H. H., Aharon, P., Carney, R., Larkin, J., and Sassen, R., (1990), Sea floor responses to hydrocarbon seeps, Louisiana Continental Slope, *Geo-Marine Letters*, **10**, 232-243.
- Sakai, H., and Matsuhisa, Y., (1996), Stable isotope geochemistry, University of Tokyo Press, 403pp.
- Sakai, H., Gamo, T., Ogawa, Y., and Boulegue, J., (1992), Stable isotopic ratios and origins of the carbonates associated with cold seepage at the eastern Nankai Trough, *Earth and Planetary Science Letters*, **109**, 391-404.
- Sakai, R., Kusakabe, M., Noto, M., and Ishii, T., (1990), Origin of water responsible for serpentinization of the Izu-Ogasawara-Mariana forearc seamounts in view of hydrogen and oxygen isotope ratios, *Earth and Planetary Science Letters*, **100**, 291-303.
- Scholle, P. A., Arthur, M. A., and Ekdale, A. A., (1983), Pelagic Environments, in Scholle, P. A., Bebout, D. G., and Moore, C. H. (eds.), Carbonate depositional environments. *AAPG Memoir*, **33**, pp 619-691.
- Shibazaki, T., and Majima, R., 1997, A fossil chemosynthetic community from outer shelf environment of the Middle Pleistocene Kakinokidai Formation, Kazusa Group in Boso Peninsula, Chiba Prefecture, central Japan, *The Journal of the Geological Society of Japan*, **103**, 1065-1080.
- Stakes, D. S., Orange, D., Paduan, J. B., Salamy, K. A., and Maher, N., (1999), Cold-seeps and Authigenic carbonate formation in Monterey Bay, California, *Marine Geology*, **159**, 93-109.
- Staudigel, H., Doyle, P., and Zindler, A., (1985), Sr and Nd isotope systematics in fish teeth, *Earth and Planetary Science Letters*, **76**, 35-44.
- Suzuki, S., Tago, Y., and Hikida, Y., (1993), Using Meigen's staining for aragonite-calcite identification in fossil molluscan shells under the scanning electron microscope, *Journal of the Geological Society of Japan*, **99**, 1-7.
- Takahashi, S., and Wada, H., (1998), Radiocarbon age determination at Shizuoka university (2), *Geoscience Reports of Shizuoka University*, **25**, 19-29, (in Japanese,

with English Abstr.).

- Takeuchi, R., Machiyama, H., Matsumoto, R., (2001), The formation process of the cold seep carbonates at the Kuroshima Knoll, *JAMSTEC Deep Sea Research*, **19**, 61-75.
- Tarutani, T., Clayton, R. N., and Mayeda, T. K., (1969), The effect of polymorphism and magnesium substitution on oxygen isotope fractionation between calcium carbonate and water, *Geochimica et Cosmochimica Acta*, **33**, 987-996.
- Tate, Y., and Majima, R., (1998), A chemosynthetic fossil community related to cold seeps in the outer shelf environment-A case study in the Lower Pleistocene Koshiha Formation, Kazusa Group, Central Japan-, *The Journal of the Geological Society of Japan*, **104**, 24-41.
- Tsuchiya, R., and Wada, H., (2002), Vacuum CO₂ extraction method from seawater for AMS ¹⁴C analysis, *Geoscience Reports of Shizuoka University*, **29**, 113-118, (in Japanese, with English Abstr.).
- Veizer, J., (1983), Chemical diagenesis of carbonates: theory and application of trace element technique, chapter 3, in Arthur, M. A. et al., eds, Stable isotopes in sedimentary geology, *SEPM short course notes 10*.
- Wada, H., Niitsuma, N., and Saito, T., (1982), Carbon and oxygen isotopic measurements of ultra-small samples, *Geoscience Reports of Shizuoka University*, **7**, 35-50, (in Japanese, with English Abstr.).
- Wada, H., Fujii, N., and Niitsuma, N., (1984), Analytical method of stable isotope for ultra-small amounts of carbon dioxide with MAT 250 mass-spectrometer, *Geoscience Reports of Shizuoka University*, **10**, 103-112 (in Japanese, with English Abstr.).

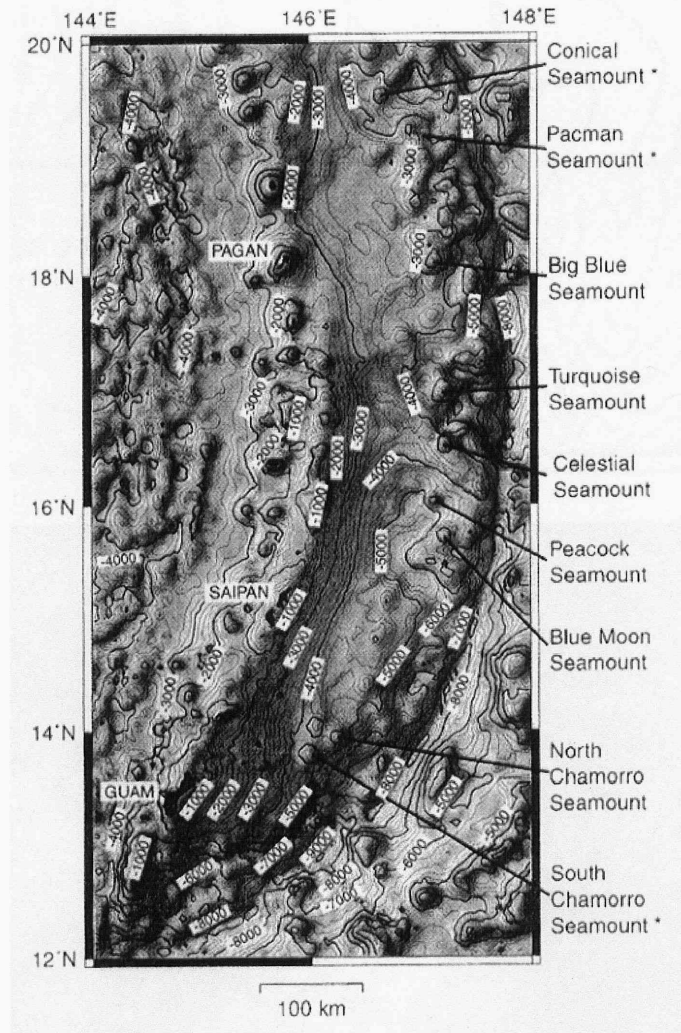


Figure 1. Detail index map of Conical Seamount and relief-shade contoured bathymetry of Mariana Forearc. Seamounts with name are mud volcanos developed at this region. Contour interval is 200m. After Fryer et al. (1999).

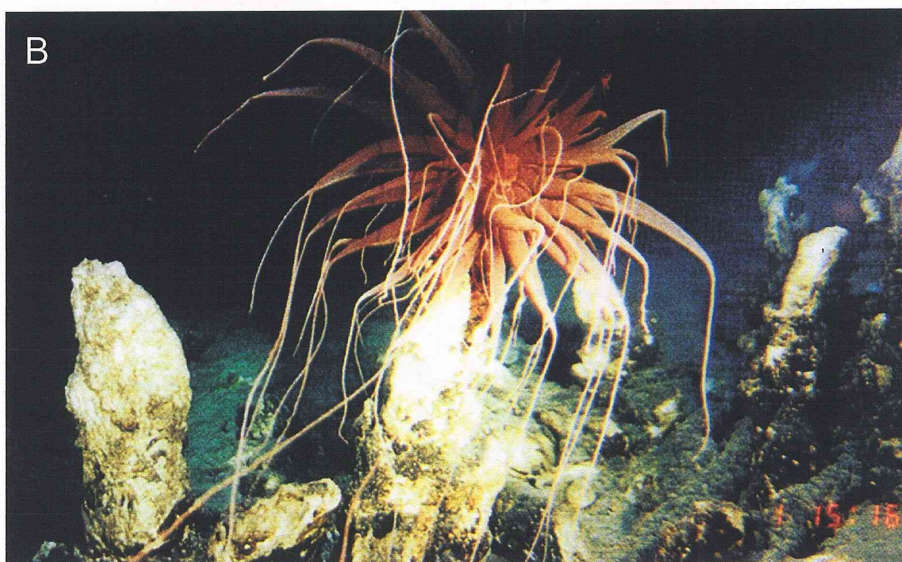
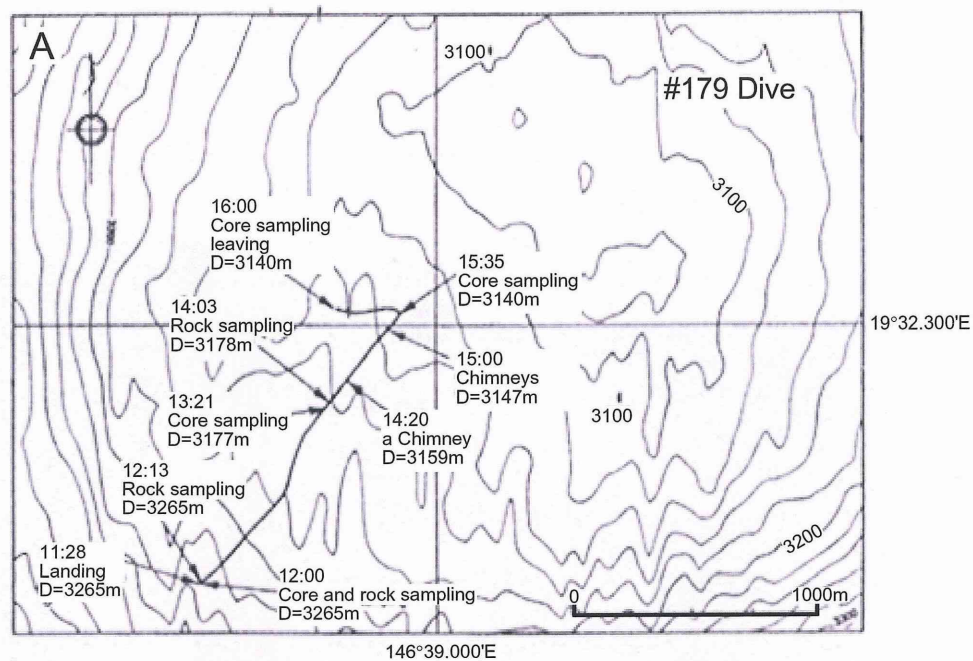


Figure 2. Ships track and occurrence of carbonate chimney on the Conical Seamount. (A): Ships track of "Shinaki 6500" on the Conical Seamount. The carbonate chimney of this study was collected at site of 14:20, 3159m in water depth. After Fujioka et al. (1994). (B): This picture was taken by "Shinkai 6500" at site of 15:00, 3147m in water depth. These chimneys in this picture and chimney of this study is different, please see figure caption 2-A. Rising upward materials are carbonate chimneys and these are arrange to linear. Sea-anemone showing red color with chimney was observed by D.S.R.V. "Alvin" in six year ago. After Fujioka et al. (1994).

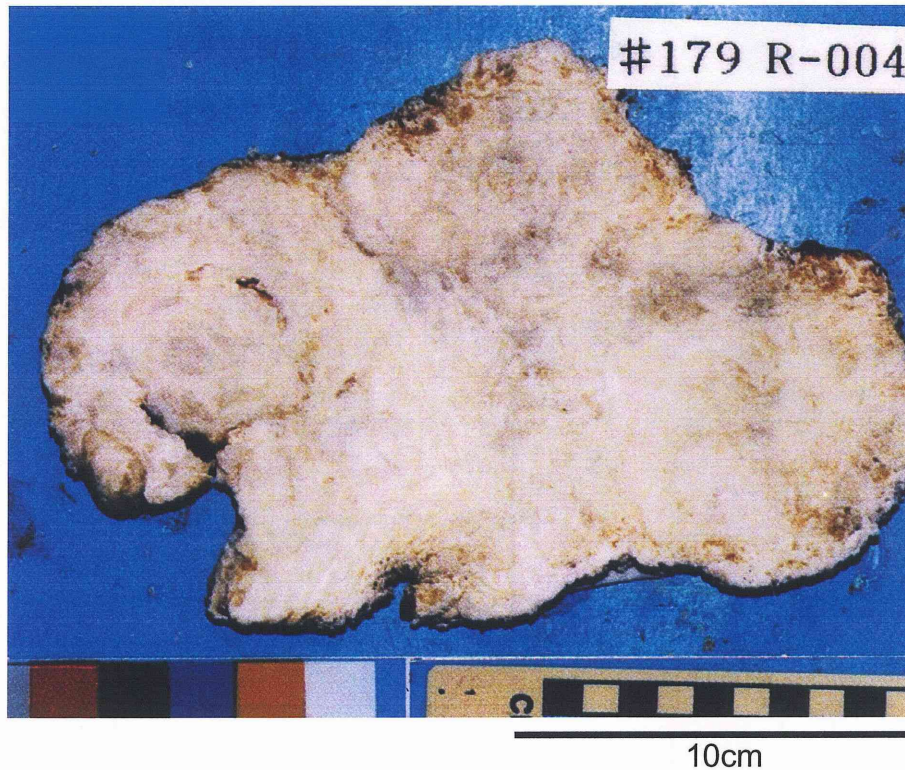


Figure 3. Cross cut surface of chimney just after collected by "Shinkai 6500". This chimney sample does not have any conduit structure for channel of venting fluid. Maximum diameter is ~20cm.

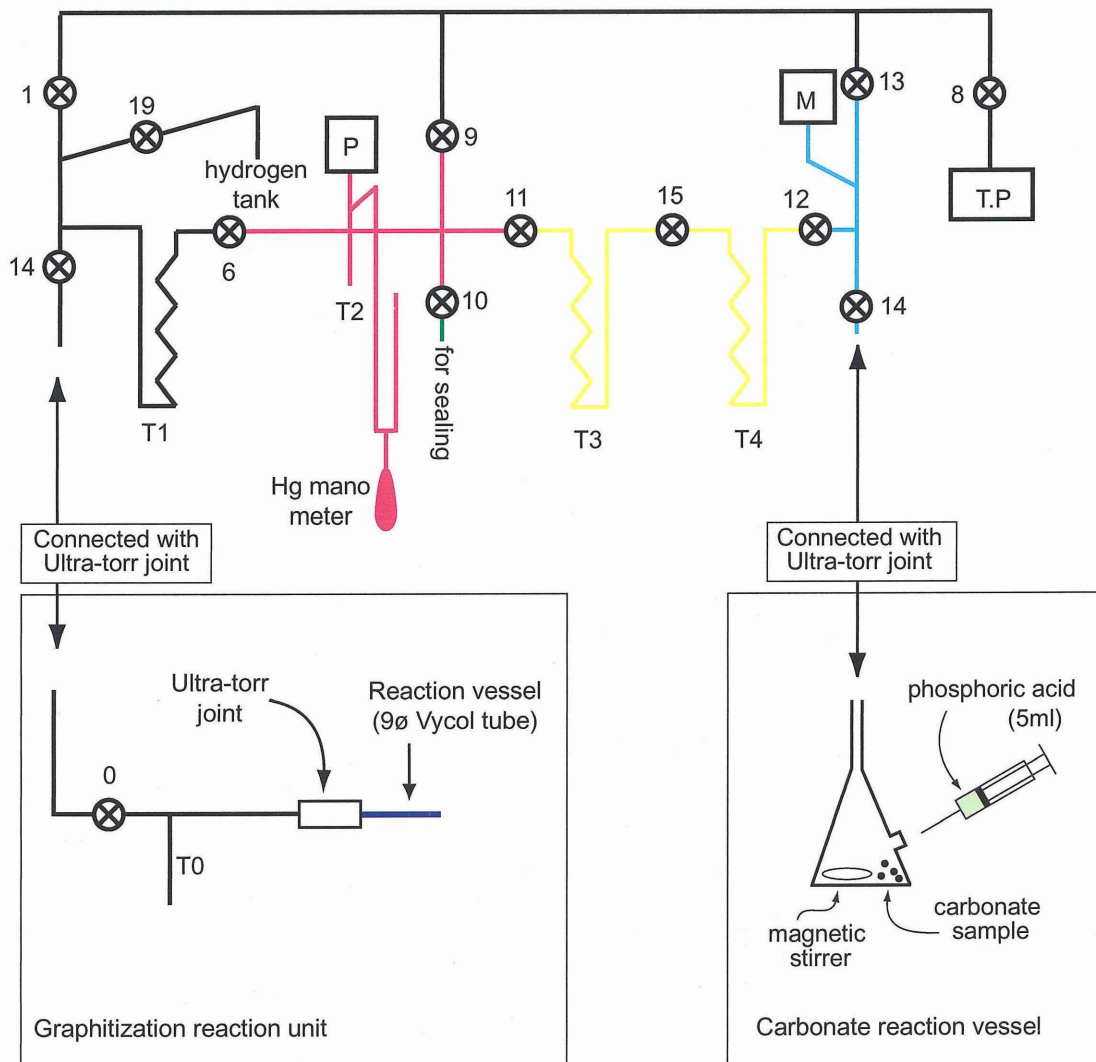


Figure 4. Outline of vacuum glass line for sample preparation of radiocarbon measurement. Glass line is composed of four functional part, gas introduce part (blue), cryogenically purification part (yellow), gas volume measurement part (red), sealing part (green). The circles with number are stop cock valve, prefixed "T" to number is cold trap. "P" and "M" is pressure gauge and each gauge corresponds to pirani gauge and capacitance manometer.

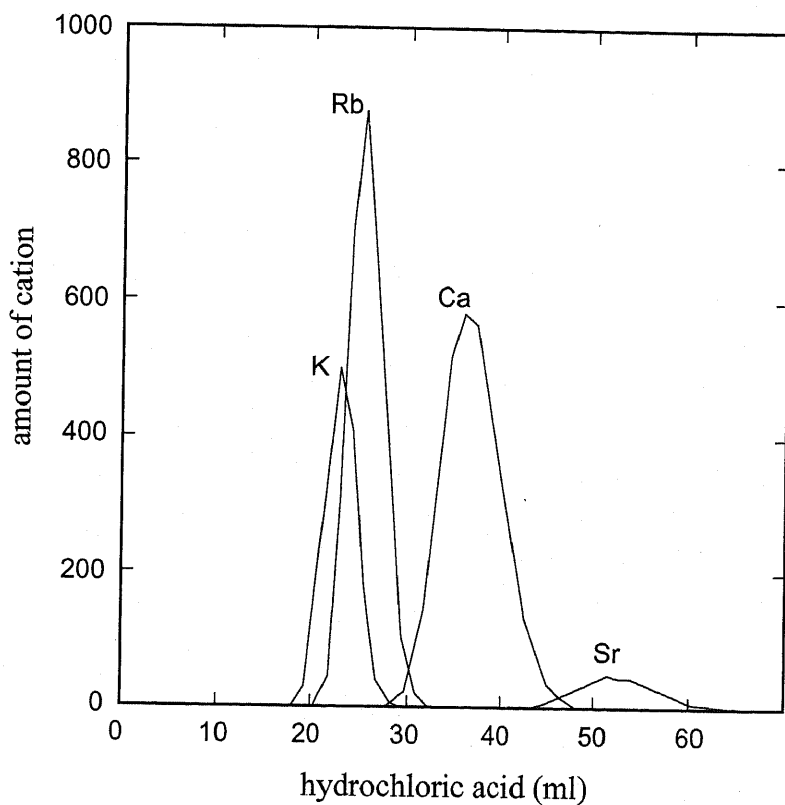


Figure 5. Calibration curve for recovery of strontium in ion-exchange resin. Horizontal and vertical axis shows amount of hydrochloric acid and amount of cation released from ion-exchange resin. When 46ml of hydrochloric acid through the resin, strontium ion escape from ion-exchange resin. This diagram was made by Mr. Tsuboi in 16 November, 2001 at Nagoya University.

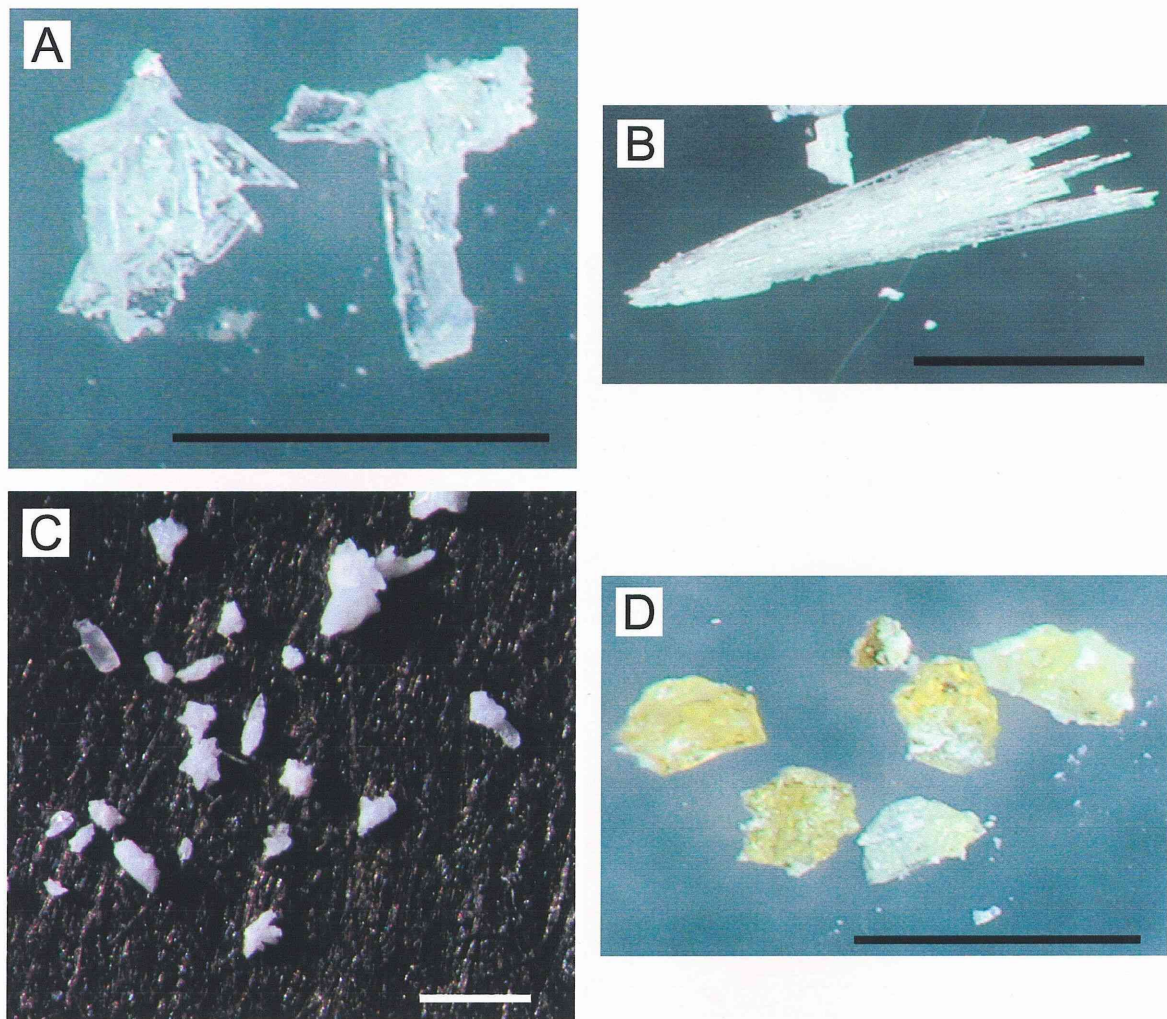


Figure 6. The grains are composed of carbonate chimney taken by KEYENCE microscope except for (C), which was taken by digital camera. (A) shows the plate-like shape and mineral phase was unknown, (B) is needle and prismatic grains (C) was mainly composed of chimney sample. Only (D) type grain has color. Scale bar in each figures are 500 μ m.

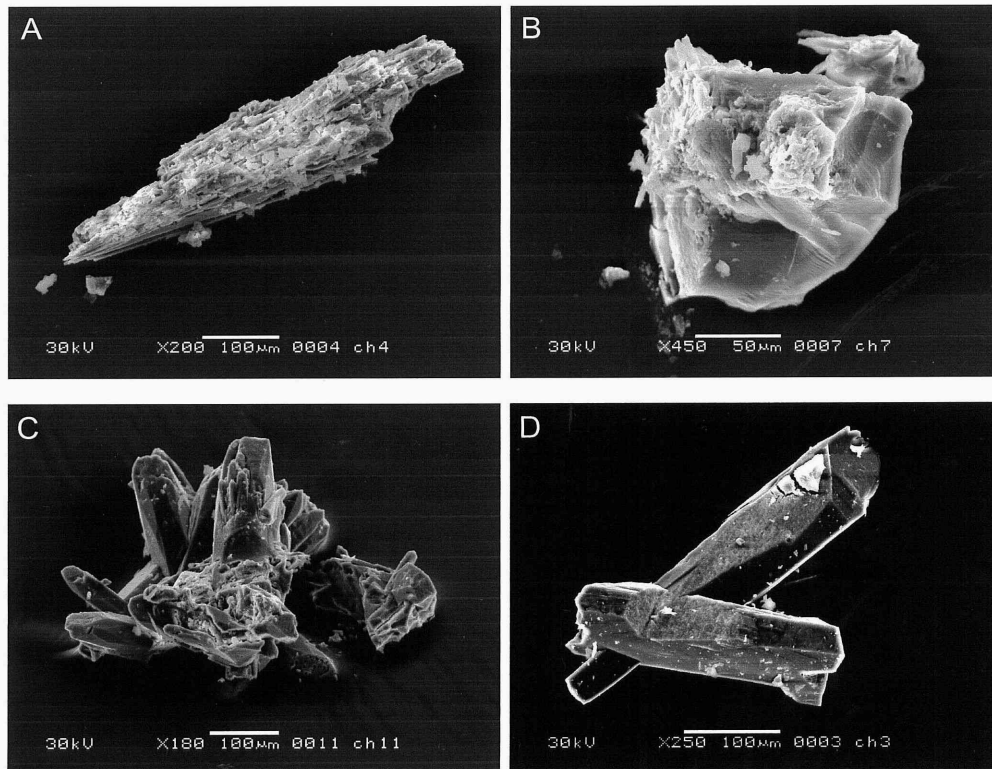


Figure 7. SEM image of two types of grains collected from the carbonate chimney.

A needle shape grain and its clusters (A) with white to translucent color, scale bar is 100µm. Figure 7-B shows irregular outer shape grain with concoidal fracture and scale bar shown 50µm. A long prism grain having a hexagonal shape with white to translucent color, scale bar is 100µm.

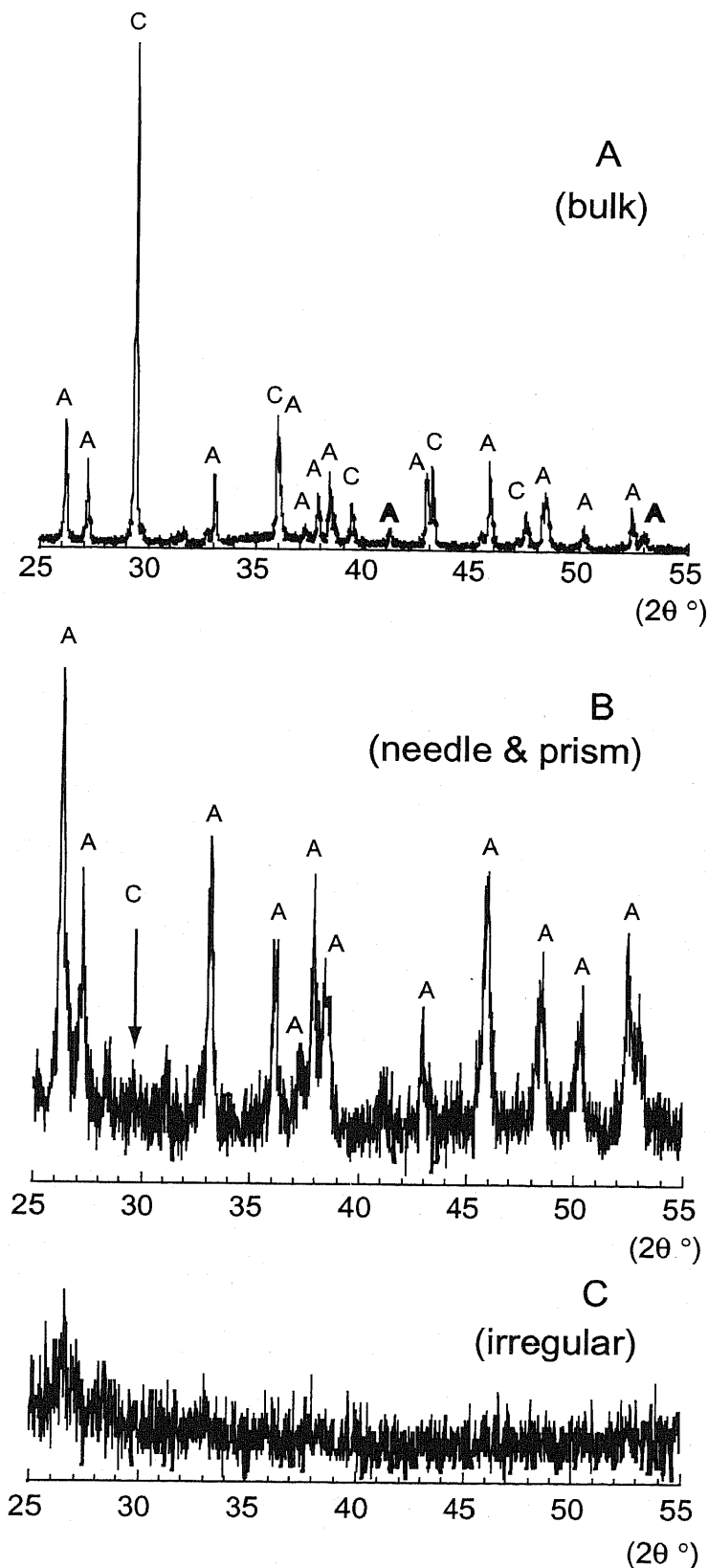


Figure 8. XRD patterns of the carbonate chimney.
 A: Bulk powdered sample of carbonate chimney. Peaks indicated by "A" and "C" correspond to aragonite and calcite, respectively. B: Peaks indicated by "A" correspond to aragonite of the needle and prism type (Fig. 1-A, 1-B). The peak with small arrow indicated by "C" would be correspond to calcite. C: Any peaked did not appear from irregular grain.

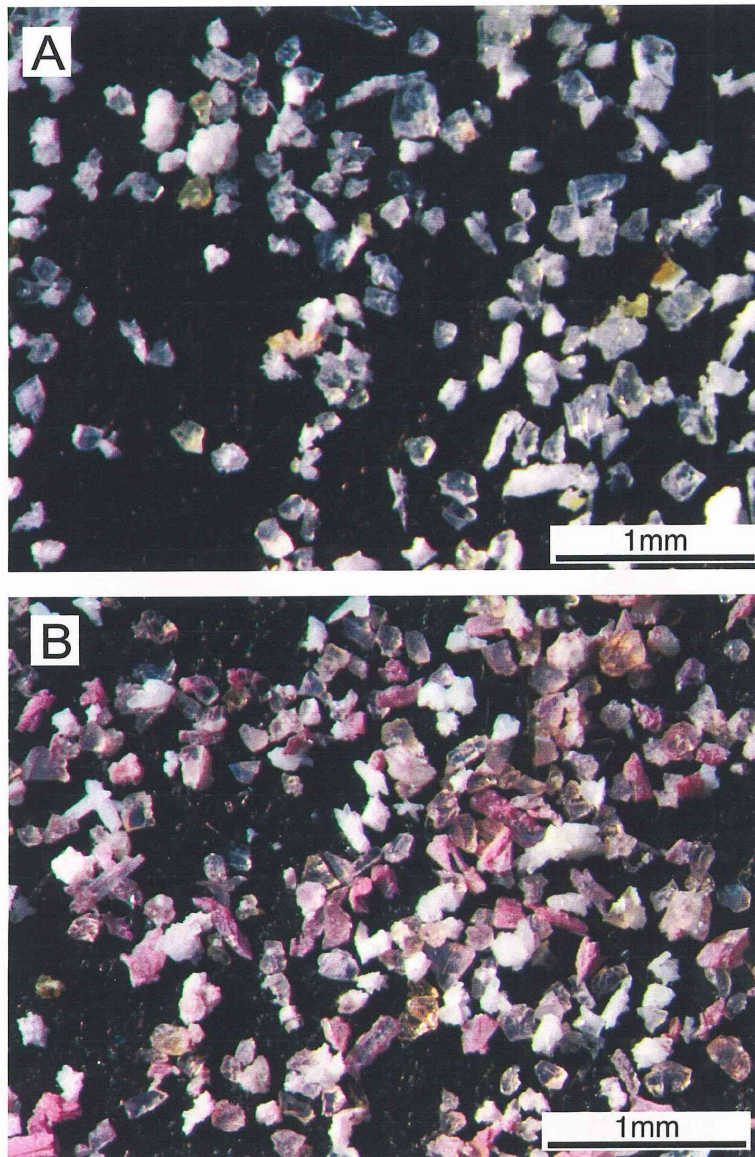


Figure 9. Figure 9-A and 9-B shows the differences of carbonate grain surface color before (A) and after (B) treated with Meigen's solution. Carbonate grains were immersed during 15 minutes at 70°C. After staining, staining solution was filter out and recovered sample was gently wash off distilled water. The grain was completely separated in stained and changeless. Scale bar was shown in each figures.

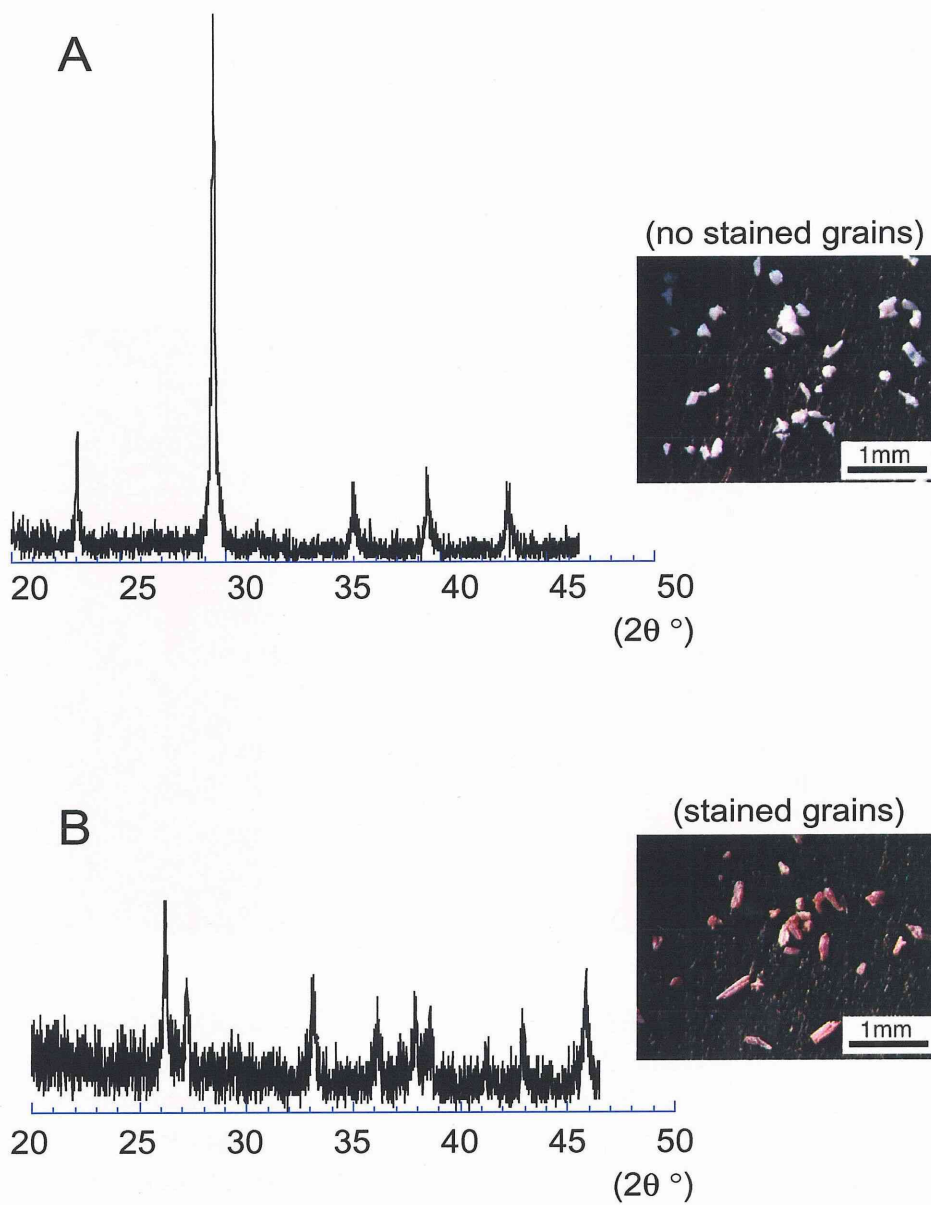


Figure 10. Chimney fragment was sieved for arrange to the same grain size, and these grains were stained by Meigen's solution under 15 minutes at 70°C. XRD results show that calcite and aragonite were completely separated in each carbonate mineral from the mixture grains. The irregular grains were easily except from mineral separation from calcite and aragonite, because these grains were unstained with Meigen's solution. All peaks displayed in A is corresponding to that of calcite and also all peaks of B show aragonite.

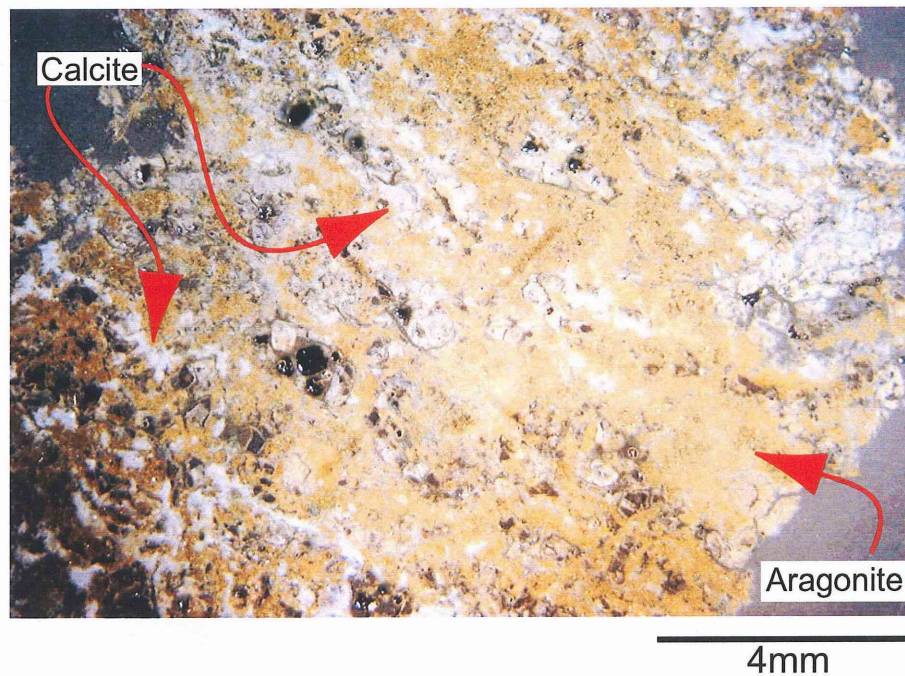


Figure 11. Occurrence of aragonite and calcite in thin section scale and this thin section was stained by Meigen's solution for calcite and aragonite identification. Meigen's solution is stained aragonite surface, calcite is changeless during staining. The pale yellowish color part shows aragonite and calcite shows the white parts. The stained color of aragonite was originally purple, but this picture was taken in later several days and its color was altered to this color.

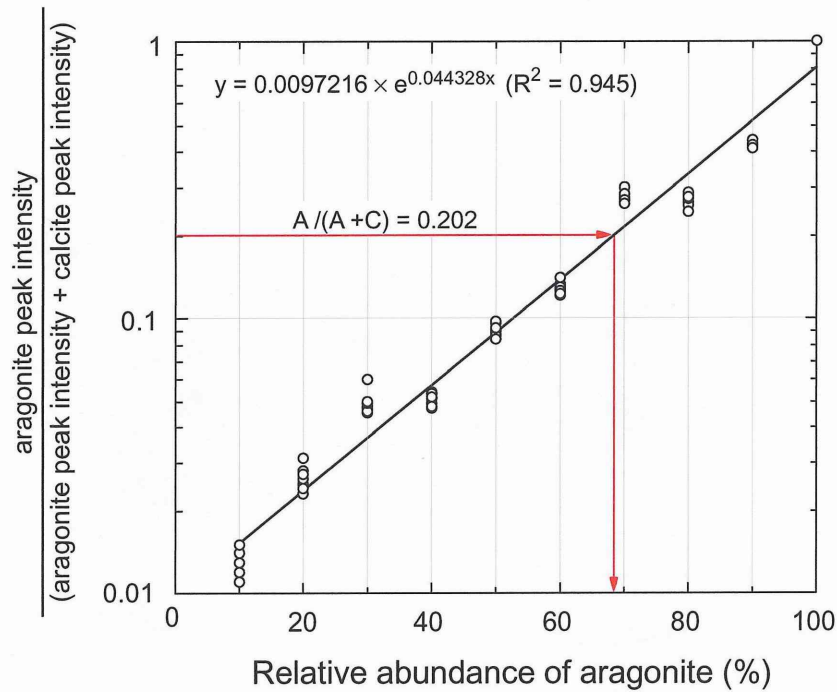


Figure 12. Estimation curve of aragonite abundance in the mixture of calcite and aragonite. This curve was made by accurate XRD analyses using calibrated sample by the adjusted known aragonite ratio sample. The ratio of aragonite peak intensity as 0.202 were calculated from the bulk XRD result shown Figure 8.

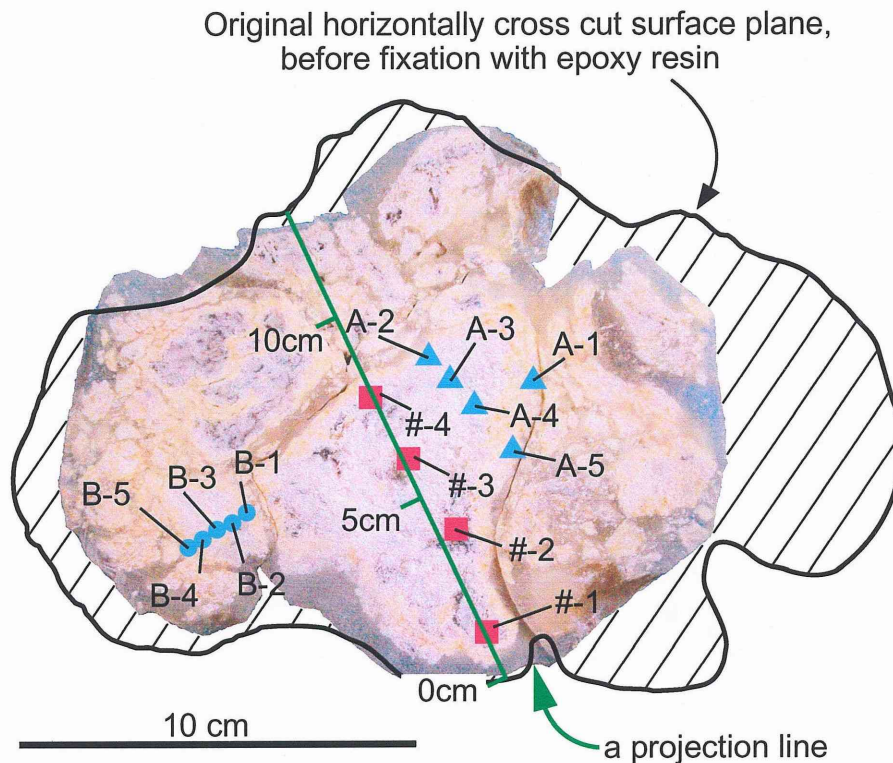


Figure 13. Sampling loci for collection of the isotopic measurements. This figure shows a horizontal cross cut surface of chimney, and striped area indicated by bold line shows the original outer shape of chimney. The outer part of this sample was broken. Only the central part of chimney was immersed with epoxy resin. Maximum diameter of chimney is about 25cm. Isotopic analyses of bulk samples collected from A-2 to A-5 and B-1 to B-5. Aragonite and calcite indicated by #-1 and #-4 were separated by hand picking using Meigen's solution. And then isotopic analyses were carried out in each mineral species. A projection line was drawn two sampling points (#-1 and #-4).

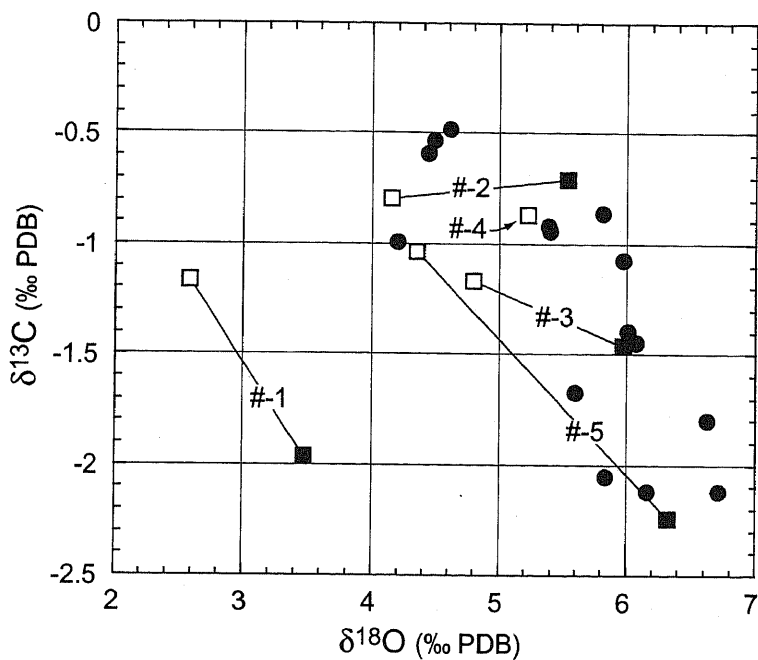


Figure 14. Diagram of $\delta^{13}\text{C}$ vs. $\delta^{18}\text{O}$ of carbonate chimney. The plots tied line show isotopic results of coexisting aragonite (open squares) and calcite (solid squares) in the same sampling position. Coexisting minerals were separated by using staining. # with numbers show sampling position and its position corresponds to figure 13. #4 is composed of only aragonite. Whereas solid circles show isotopic results of bulk condition. All isotopic data are listed in Table 1.

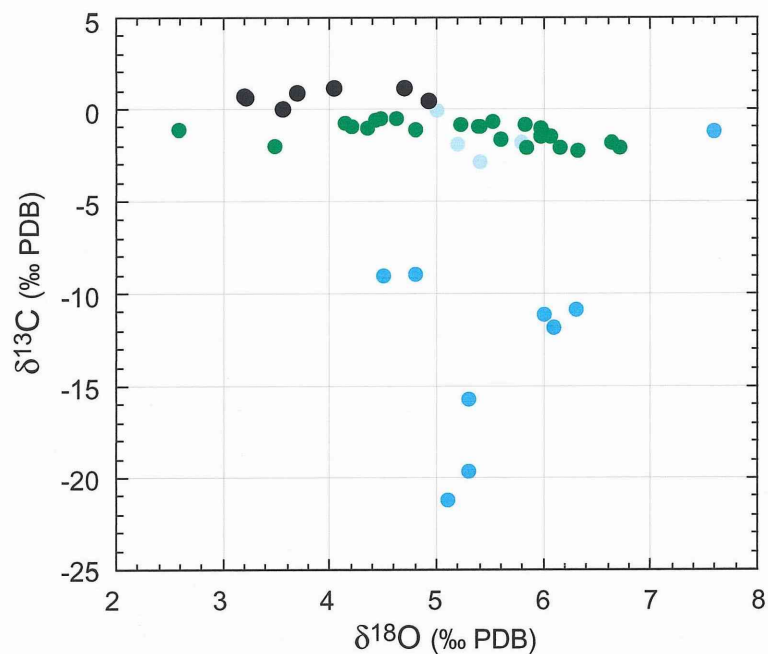


Figure 15. Diagram of $\delta^{13}\text{C}$ vs. $\delta^{18}\text{O}$ of aragonite observed in serpentinized peridotite in fracture zone (black circles, Bonatti et al., 1980) and carbonate recovered from Mariana Forearc (other color circles). Bonatti et al. (1980) suggested that aragonites (black circles) were precipitated during reaction between ultramafic rocks and circulating seawater and these aragonites were originally seawater. Chimney of this study represents green circles. Pale blue circles show previous results of chimney from Conical Seamount (Haggerty, 1991). Blue circles show results of radial acicular bundles of aragonite in the sediment dredged from Chamorro Seamount located at $13^{\circ}46'\text{N}$, $146^{\circ}04'\text{E}$ in Mariana Forearc (Haggerty, 1987; 1991) and its grain size is a few millimeter scale.

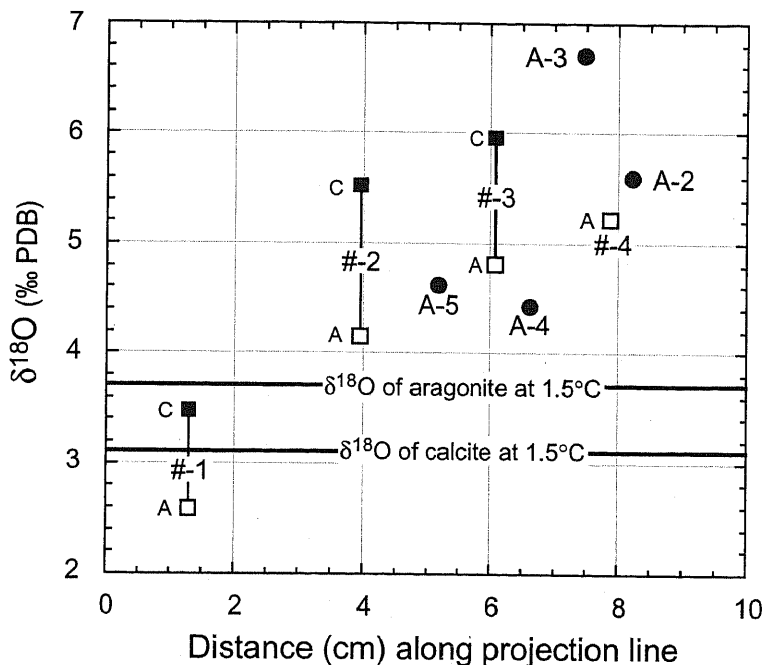


Figure 16. Relationship between $\delta^{18}\text{O}$ value of carbonate chimney and the sampling loci measured along the projection line corresponding to Figure 13. The tie lines show the isotopic results of coexisting calcite and aragonite in each sampling loci. #-4 is composed of only aragonite. Open and solid squares indicated by "A" and "C" correspond to aragonite and calcite, respectively. Solid circles show the results of bulk sample value (A-2 to A-5). Two horizontal bold lines show the oxygen isotopic values of calcite and aragonite precipitated from seawater (0‰) at 1.5°C. These precipitation temperature were calculated from the equation given by O'Neil et al. (1969) and Tarutani et al. (1969).

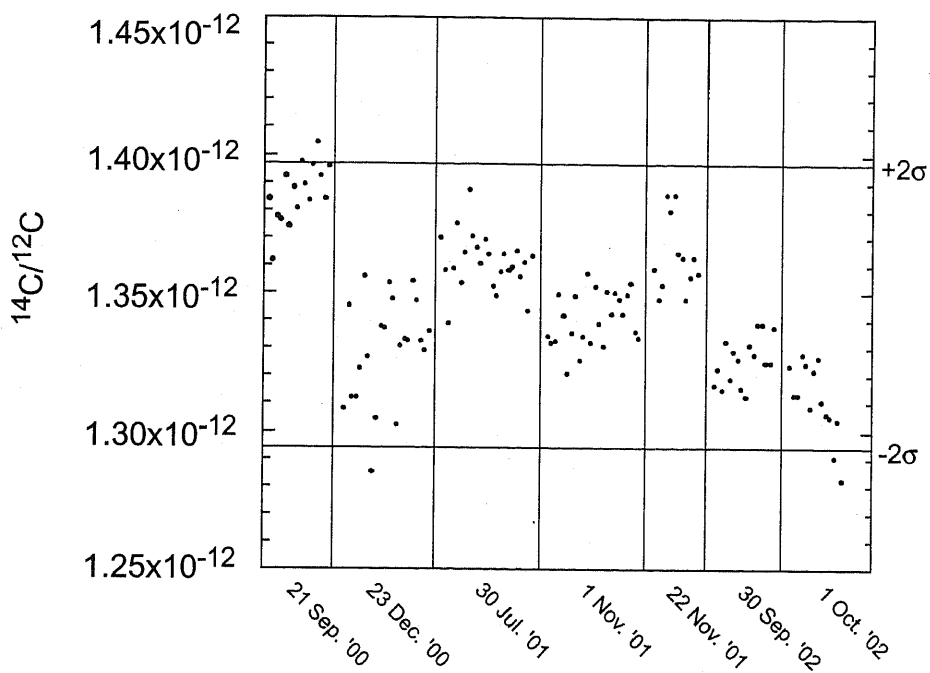


Figure 17. $^{14}\text{C}/^{12}\text{C}$ variation of standard sample (SRM-4990C) measured by AMS. Horizontal axis shows the date of radiocarbon measurement for our laboratory samples.

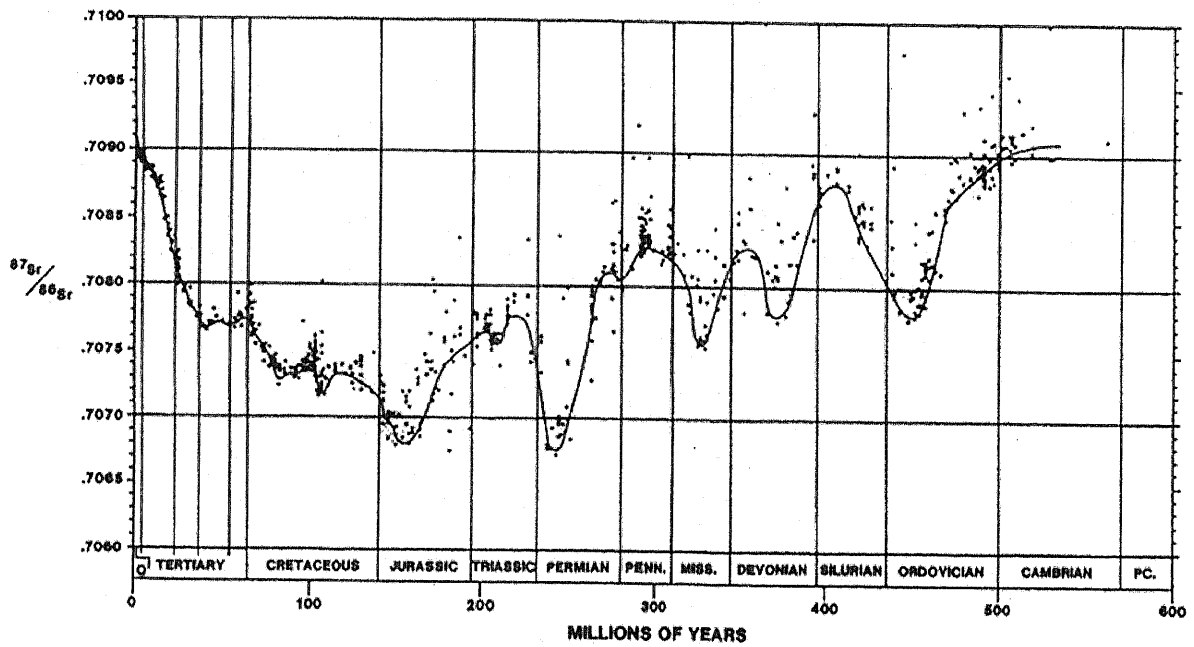


Figure 18. Plot of $^{87}\text{Sr}/^{86}\text{Sr}$ ratio through a Phanerozoic. Line respects best estimate of seawater ratio versus time. After Burke et al. (1982).

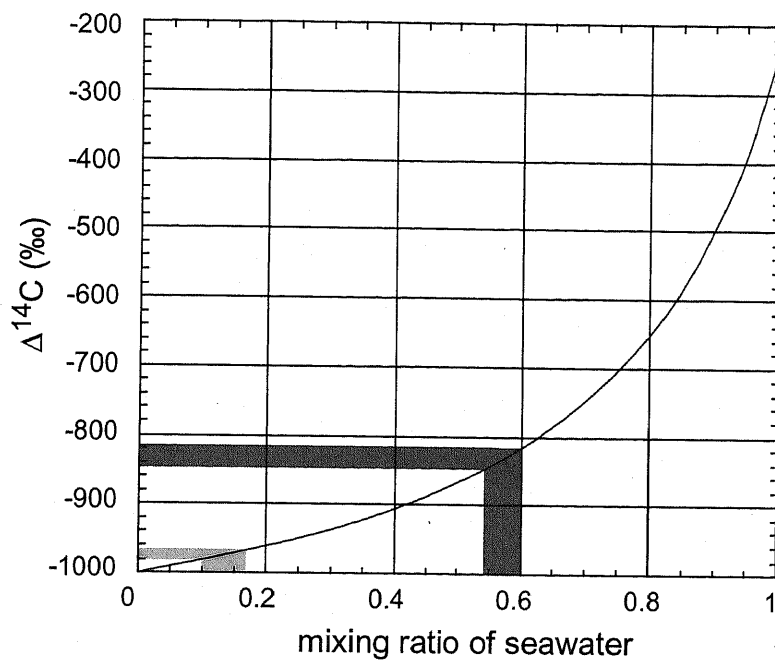


Figure 19. Mixing ratio calculated from radiocarbon activity. Horizontal dark and light gray band shows the radiocarbon activity value of aragonite and calcite, respectively. Concerning a simple mixing of these fluid, aragonite was precipitated at 60% of seawater, whereas calcite was precipitated at 10% of seawater. Mixing curve was assumed that two end-member, seawater to be -240‰ and 2mmol/l and the venting fluid to be -1000‰ and 9.3mmol/l .

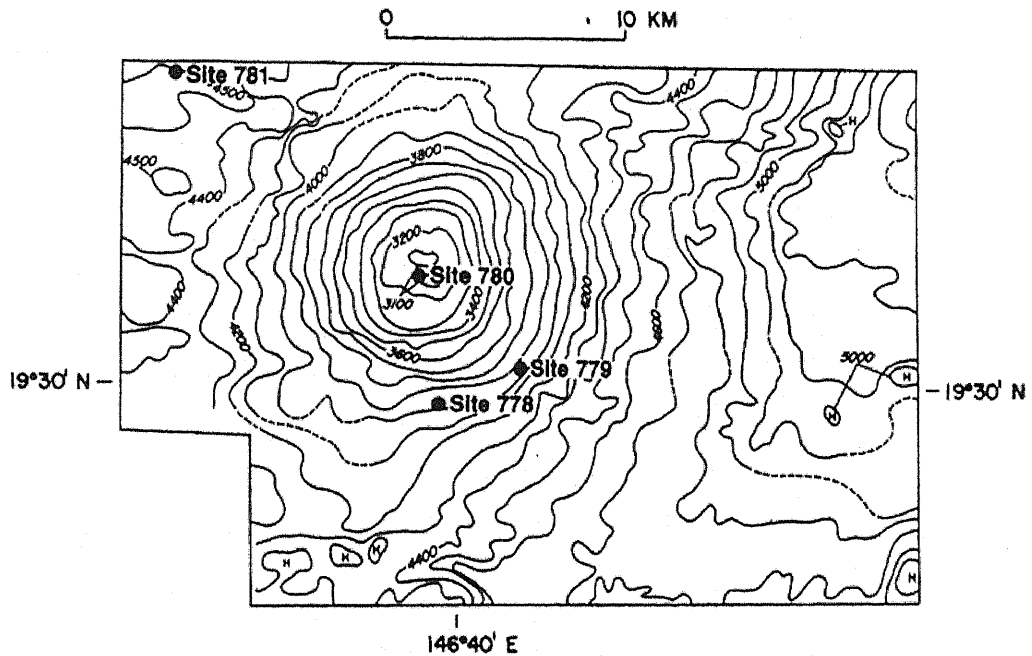


Figure 20. Bathymetry of Conical Seamount showing locations of Ocean Drilling Program Leg 125, site 778 through 781. Countour intervals are 1000m. After Mottl(1992).

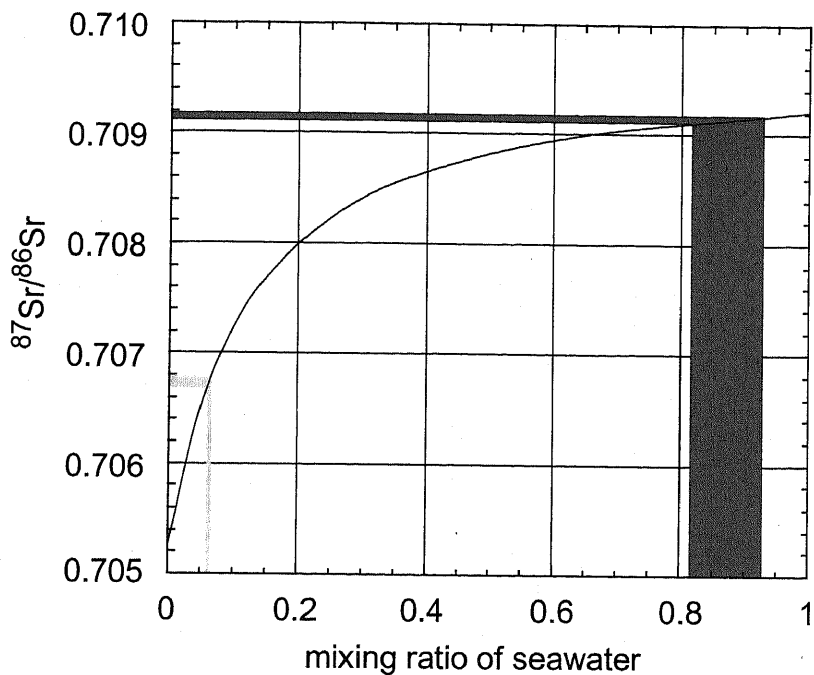


Figure 21. Mixing ratio calculated from Sr isotopic results. Horizontal dark and light gray band shows the Sr isotopic value of aragonite and calcite, respectively. Concerning a simple mixing of these fluid, aragonite was precipitated at the high seawater ratio of ~90%, whereas calcite was precipitated under a low seawater contribution at ~5%. Mixing curve was assumed that two end-member, average value of seawater (0.7092) and Sr isotopic value of interstitial water (0.7052) in Conical Seamount reported by Haggerty & Chaudhuri (1992).

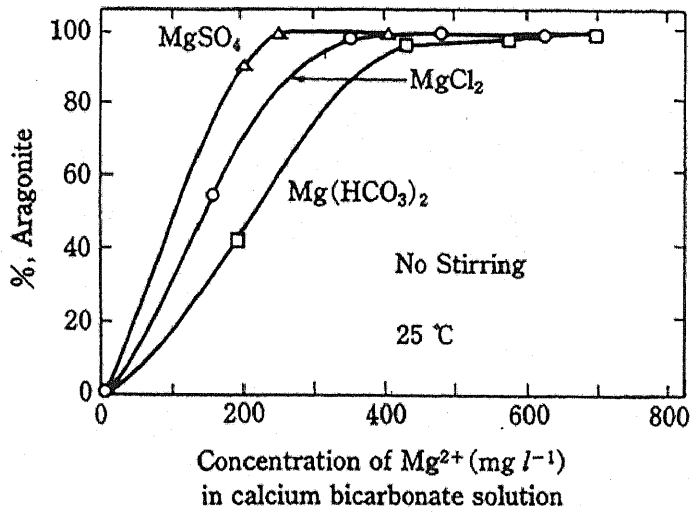


Figure 22. Experimental results of selectively aragonite precipitation in dissolved Mg^{2+} solution. After Kitano (1989).

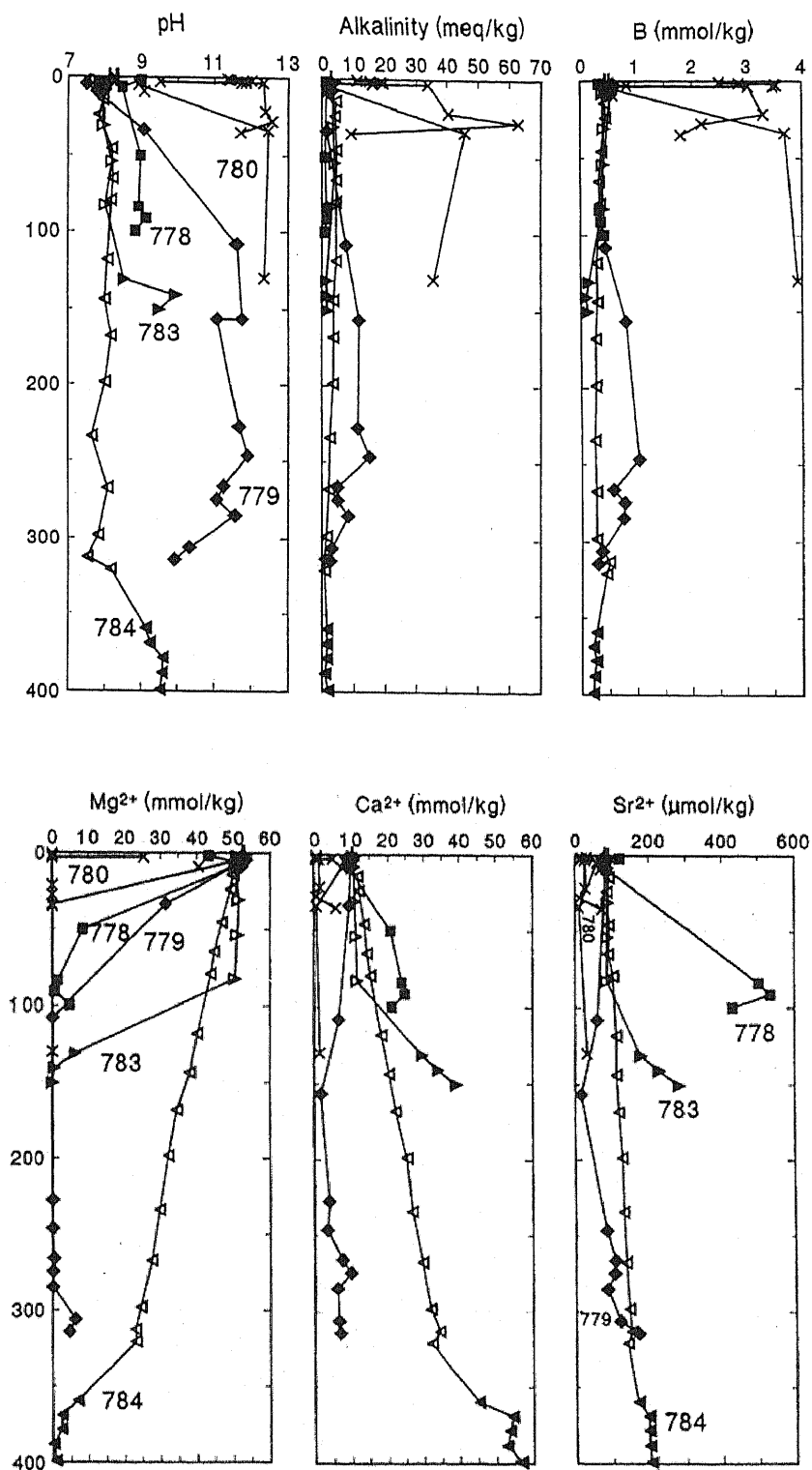


Figure 23. Composition of pore water from cores at Sites 778 (circles), 779 (diamonds), 780(crosses), 783 (right-triangles), and 784 (left-face triangles). After Mottl (1992).

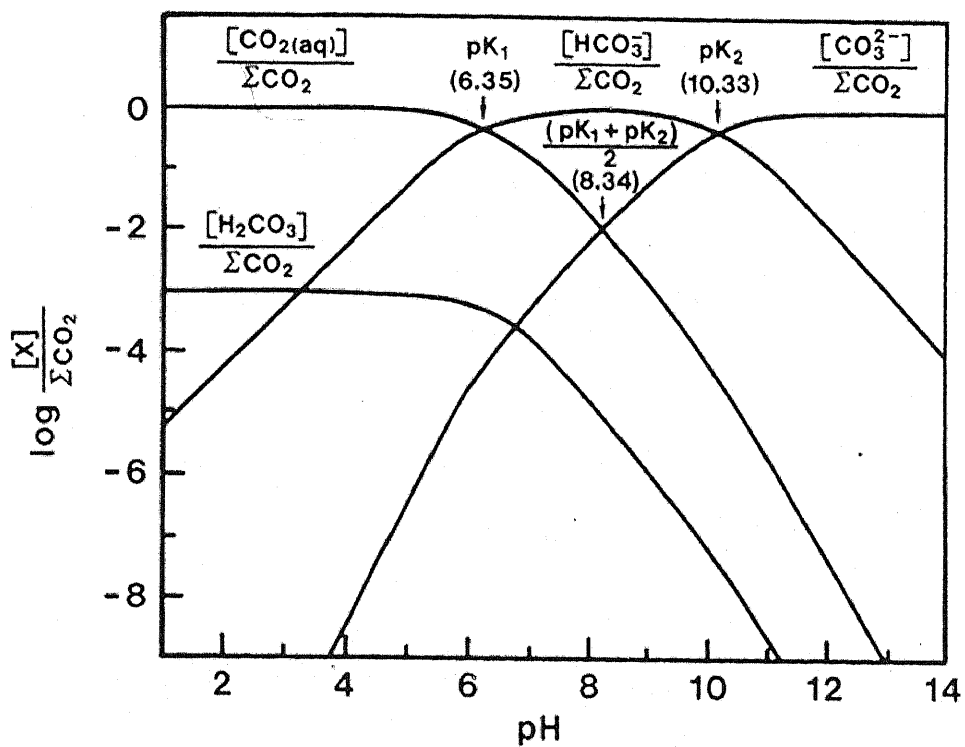


Figure 24. A Bjerrum diagram for the relative proportions of carbonic acid system chemical species as a function of pH. $\text{p}K$'s are values at 25°C . After Morse and Mackenzie (1990).

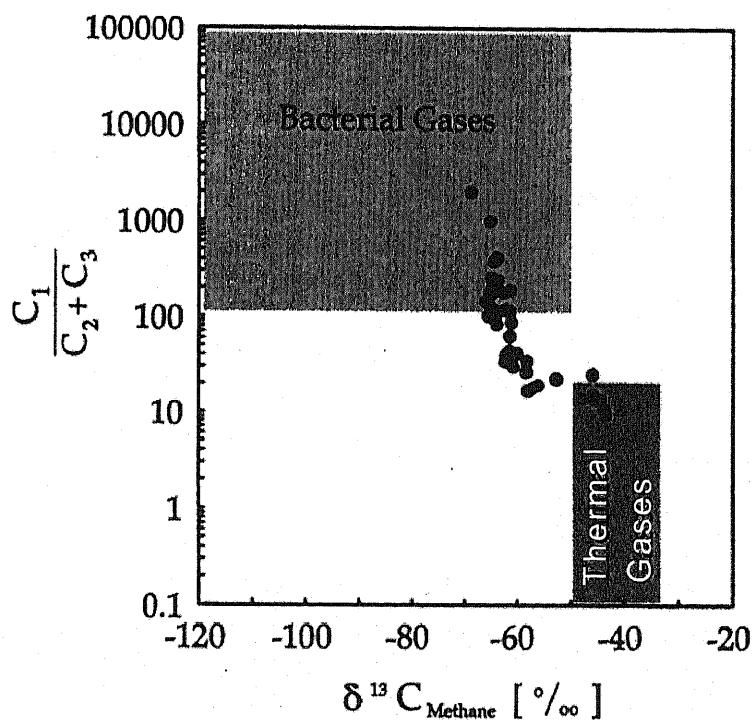


Figure 25. Carbon isotopic ratios of methane and molecular ratios. Solid circles show the example results at site 808 of ODP Leg 131, at Nankai Trough. These plots indicate mixing of bacterial and thermal gases. After Berner and Faber (1993).

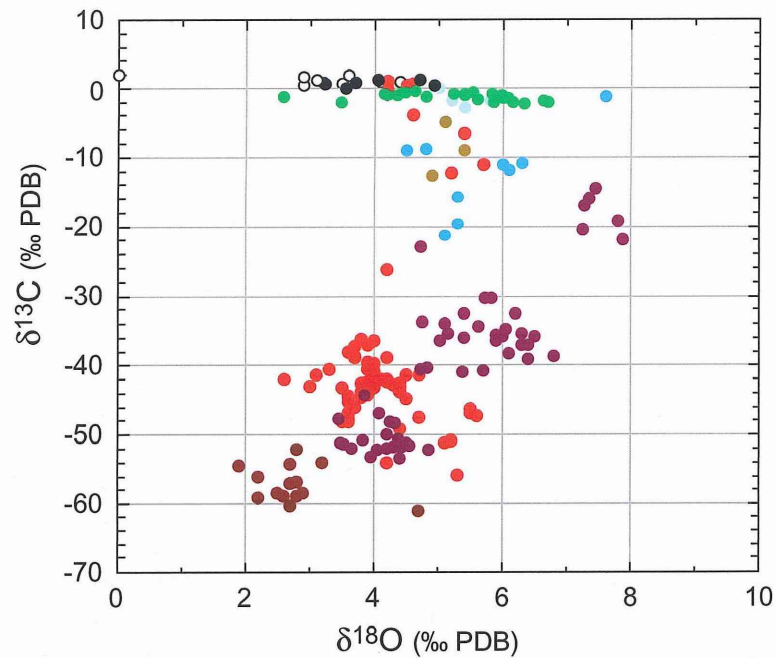


Figure 26. Diagram of $\delta^{13}\text{C}$ vs. $\delta^{18}\text{O}$ of carbonate deposits associated with cold seepage. Chimney of this study represents green circles. Pale blue circles show previous results of chimney from Conical Seamount (Haggerty, 1991). Blue circles show results of radial acicular bundles of aragonite in the sediment dredged from Chamorro Seamount (Haggerty, 1987; 1991). Black circles show aragonite observed in serpentinized peridotite at fracture zone (Bonatti et al., 1980). Open circles show aragonite observed in ultramafic rocks of site 895, ODP leg 147 at Hess deep (Früh-Green et al., 1996). Olive circles show dolomite chimney at Otago continental slope, New Zealand (Orpin, 1997). Red, purple, and brown circles show carbonate deposit precipitated from the fluid origin from methane hydrate. Red circles show result at Nankai Trough (Sakai et al., 1992), purple circles are result of Oregon off (Kulm et al., 1990), and brown circles are results of carbonates observed at offshore oil field in North Sea (Hovland et al., 1987).



Figure 27. Index map showing the location of boring survey, southern part of Yokohama City, Kanagawa Prefecture, central Japan. Location Kb is the boring site. After Tate and Majima (1998), and Kitazaki and Majima (2002).

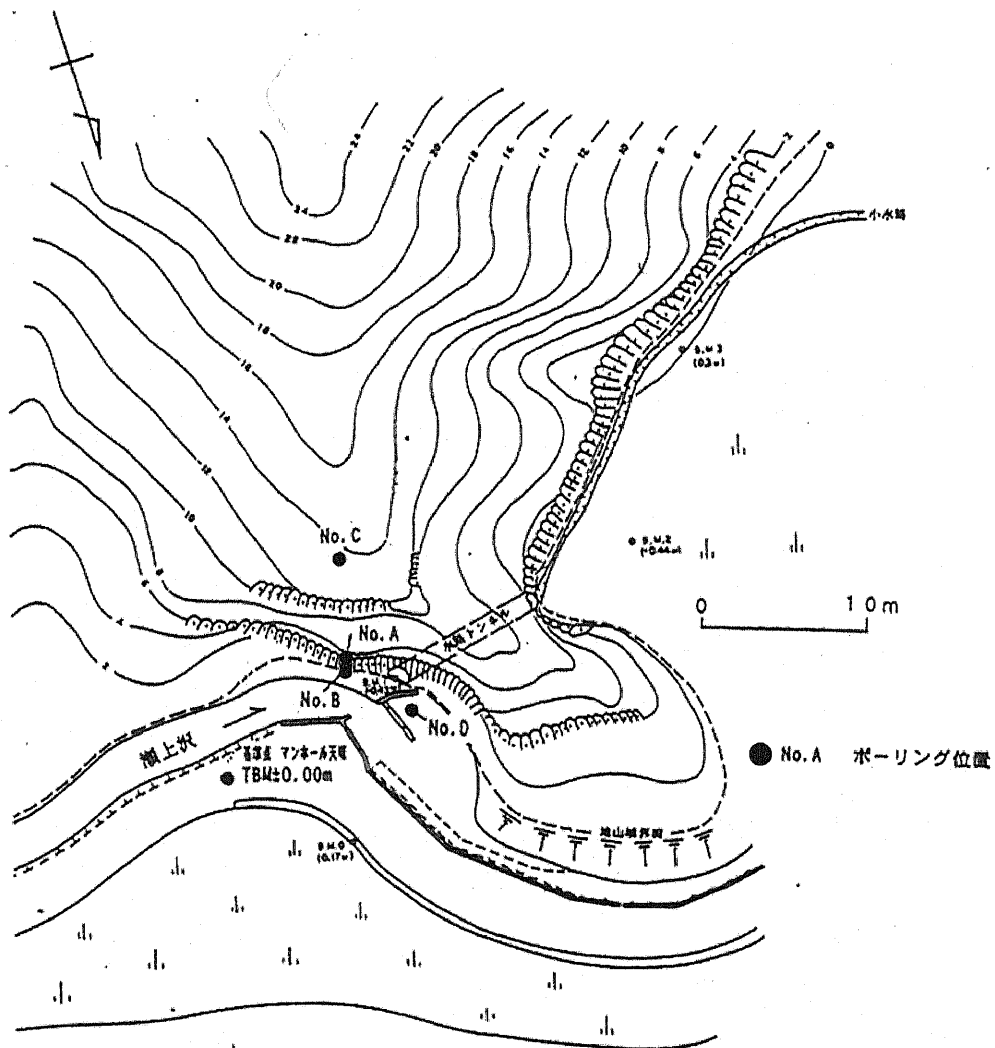


Figure 28. Detail topographic map around boring site. Four small circles with alphabet from "A" to "D" indicates boring site. Isotopic analyses were carried out in core "D"

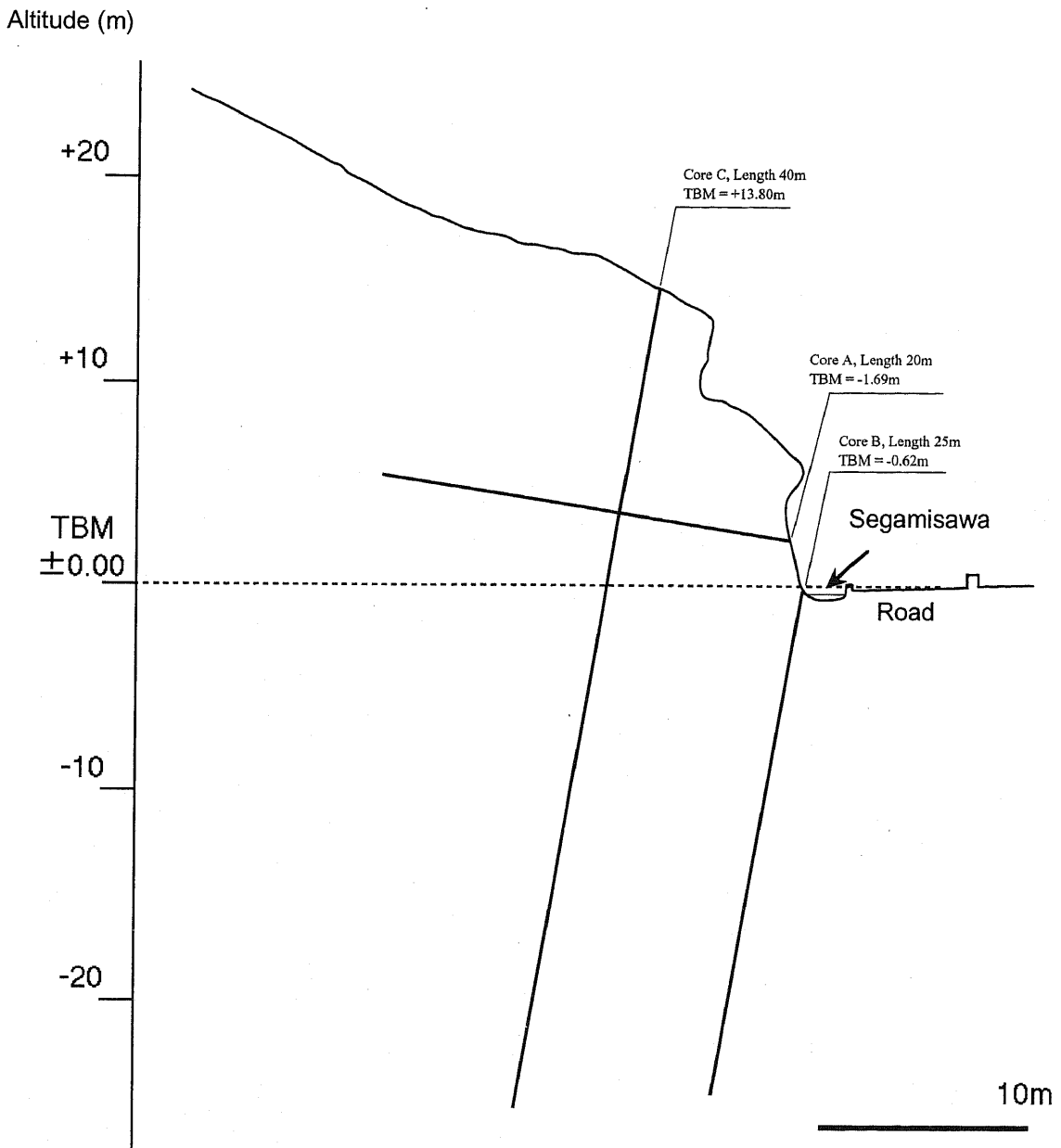


Figure 29. Cross section of boring site and position was described in Figure 24. Core A was drilled to parallel and core B to D was orthogonal to bedding plane.

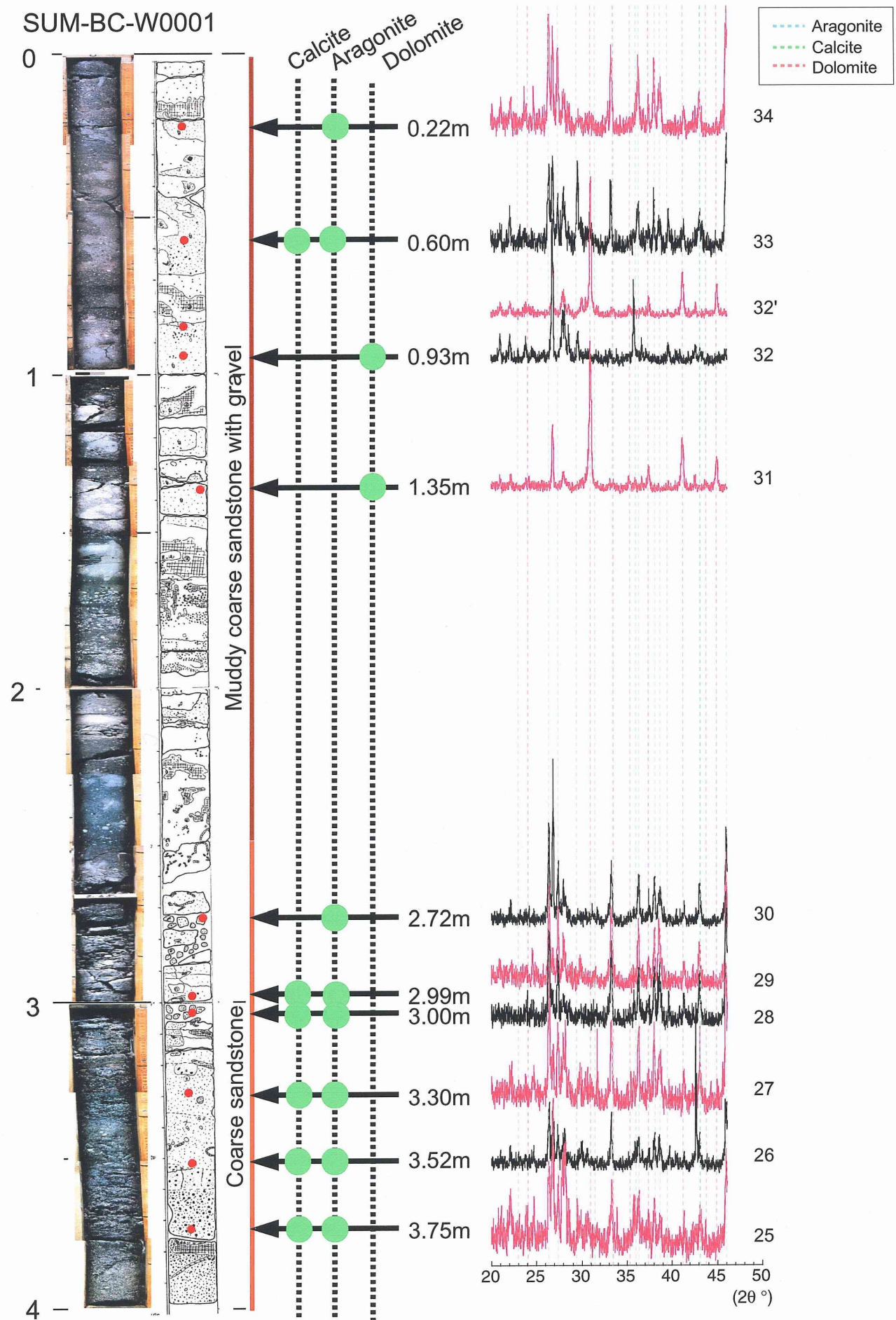


Figure 30-1

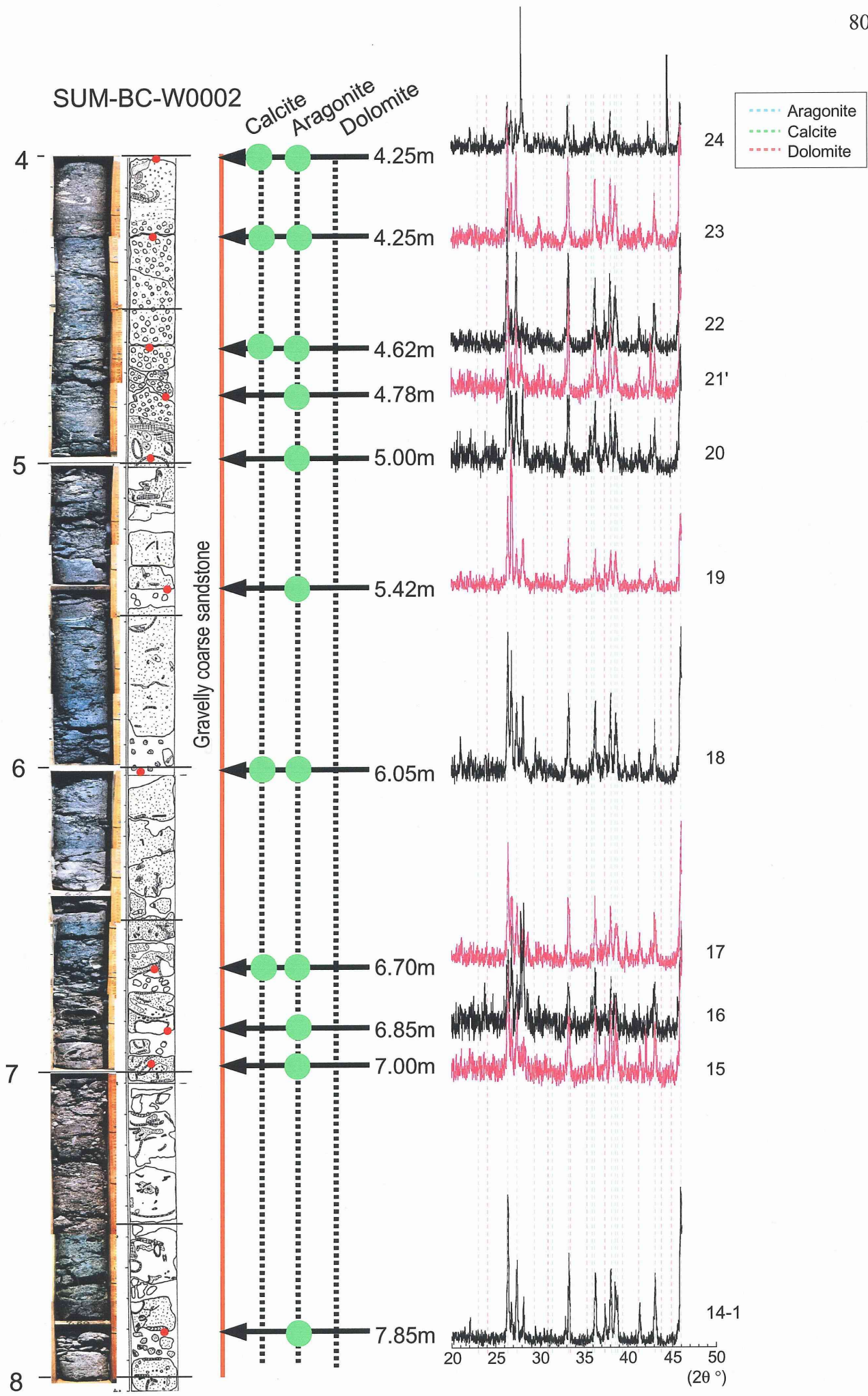


Figure30-2

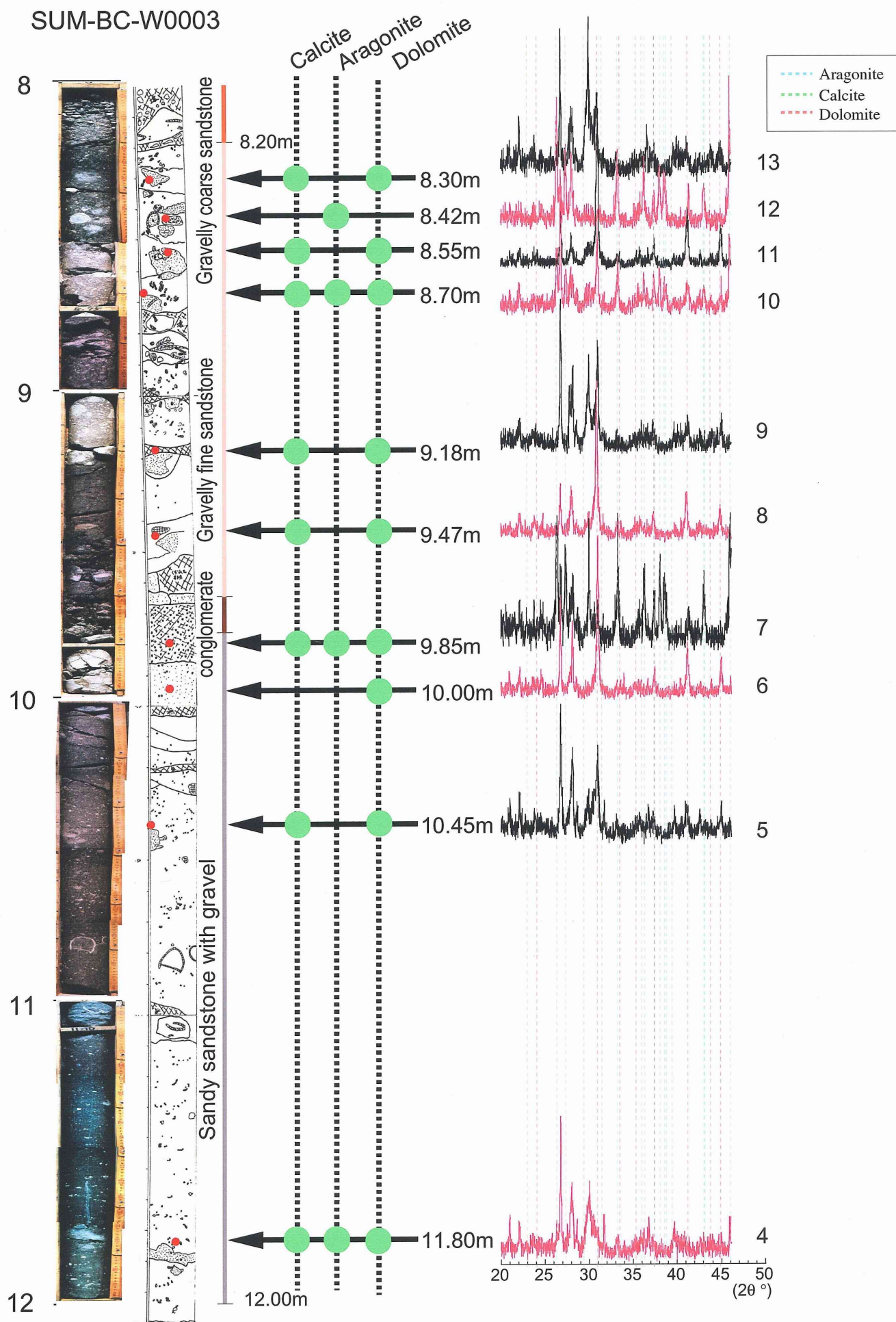


Figure 30-3

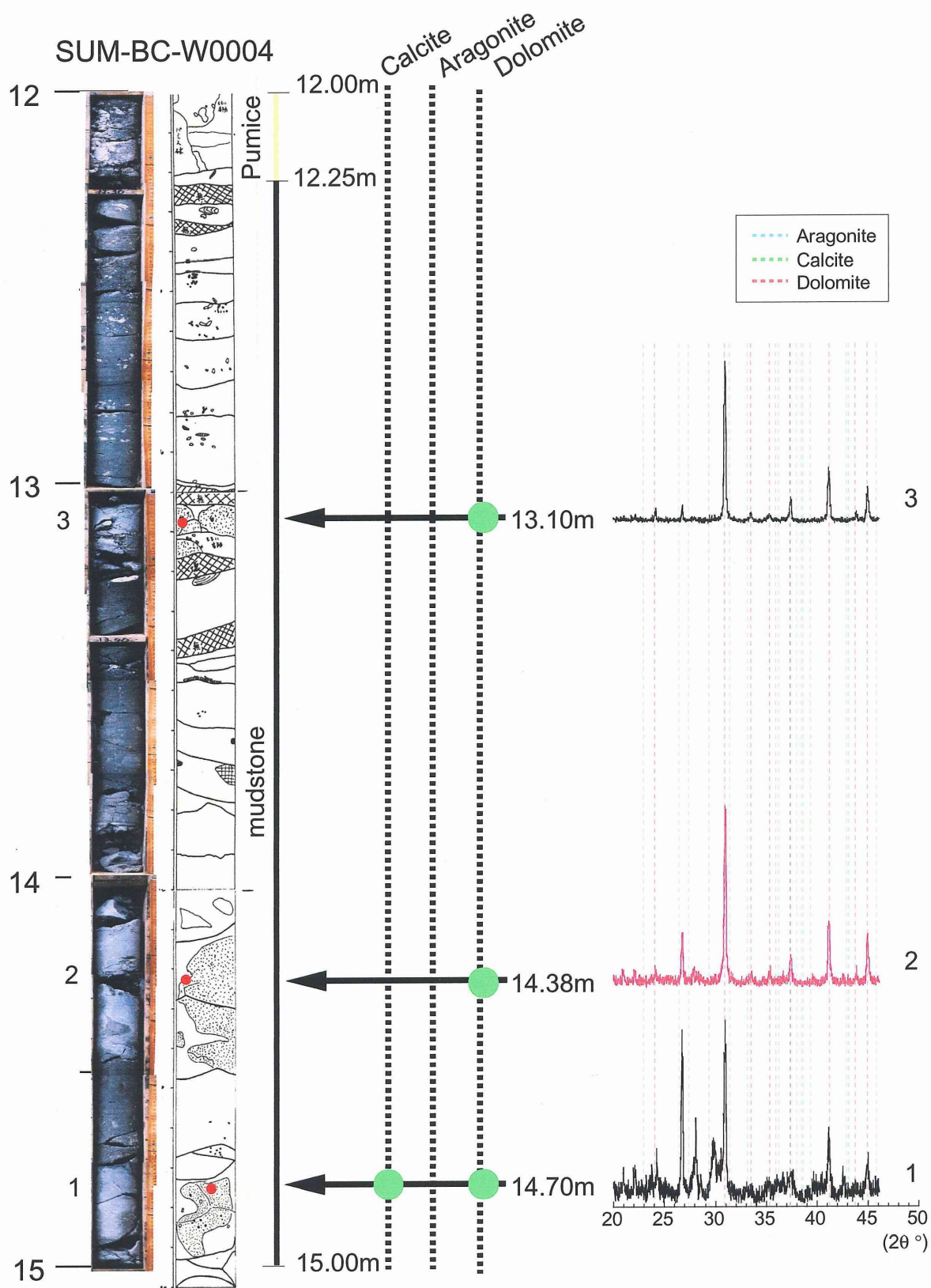


Figure 30-4

Figure 30. This figure shows the picture of core "D" and results of XRD measurements of carbonate cement. The number with core picture in left side shows the depth below the ground level (meter). Sketch to right side of core picture shows distribution of cements and valve fossils. Small red circles in sketch are sampling point of cement for isotope measurement and green circles show carbonate mineral phase in sampling point and XRD results were listed in the same figure. The upper part of core was observed aragonite and calcite assemblages, the mixture of calcite and dolomite was dominant in the lower part below 8m.

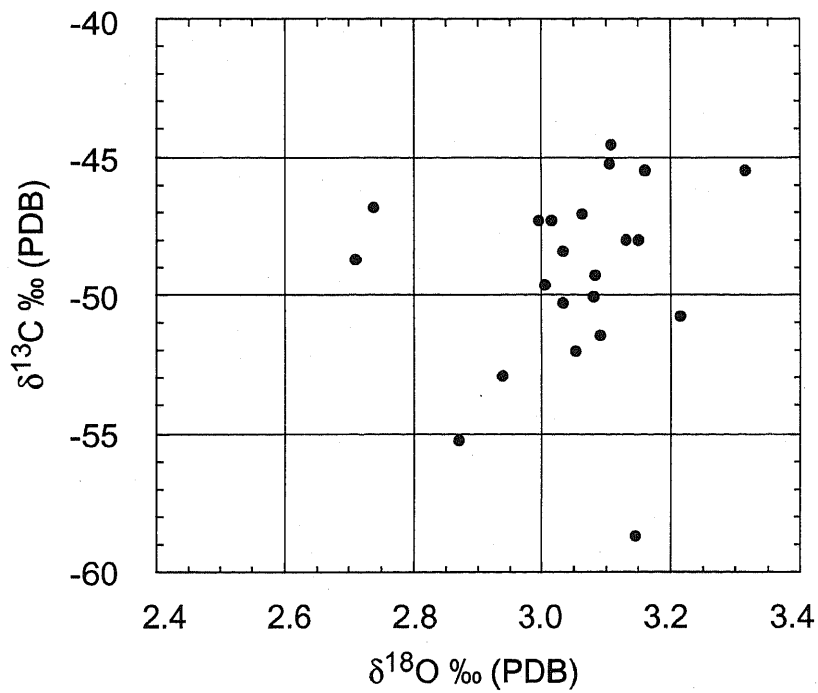


Figure 31. A diagram of carbon and oxygen isotopic values of carbonate cement collected from boring core "D". Cement was composed of aragonite, calcite, and dolomite. The upper part of core was observed aragonite and calcite assemblages, the mixture of calcite and dolomite was dominant in the lower part below 8m. This isotopic results were only shown aragonite and calcite isotopic values.

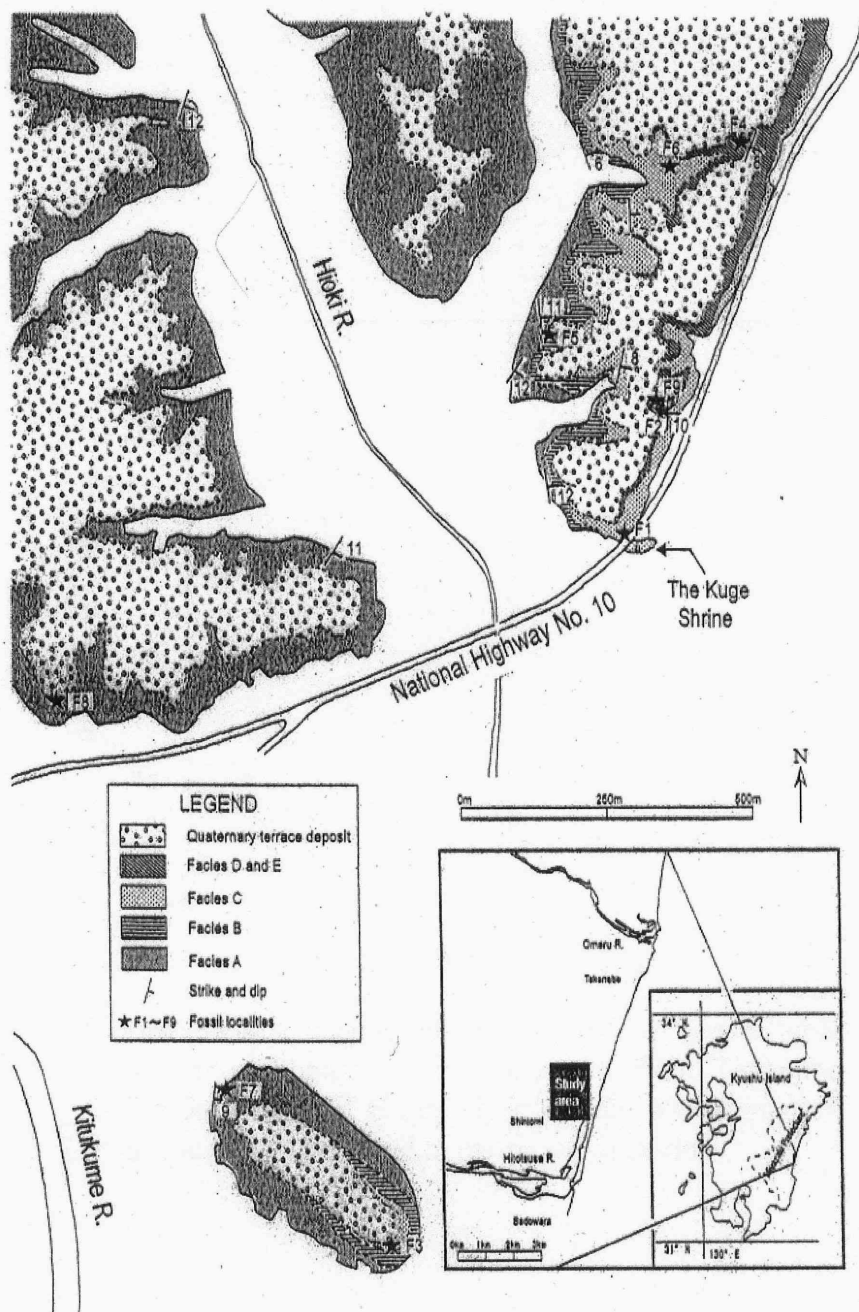


Figure 32. Index map of sampling location. Isotopic analyses were carried out in the sample collected from the Kuge Shrine, where is located at Shintomi town, Koyu Country, Miyazaki Prefecture. This area outcrop the upper part of the Upper Pliocene, Takanabe Formation of Miyazaki Group (Majima and Ikeda, 2002).

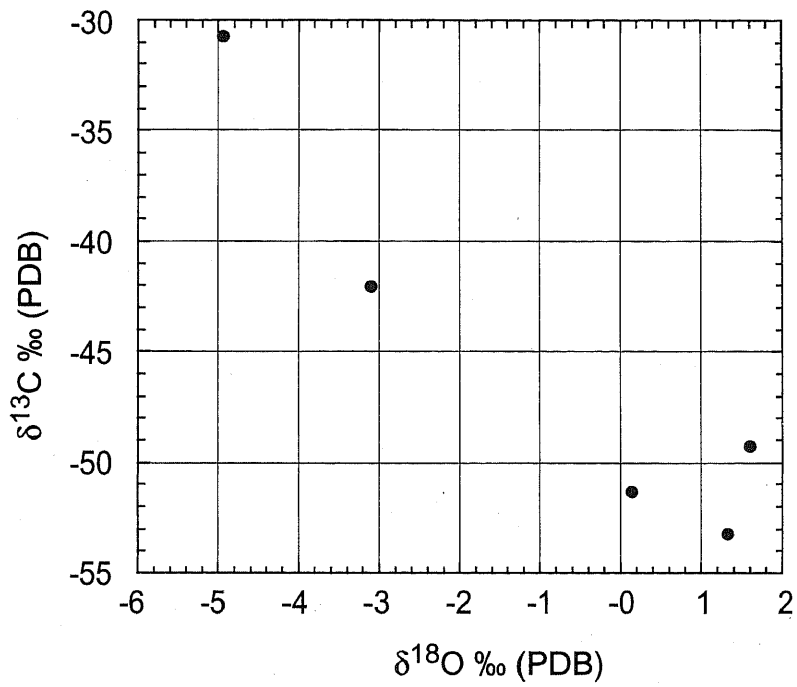


Figure 33. A diagram of carbon and oxygen isotopic values of carbonate cement collected from Takanabe formation, Miyazaki Group. This cement was composed of calcite and precipitated in matrix of sediment.

Table 1. All data for caribration of relative abundance of aragontie in calcite-aragonite mixture. These data were measured by accurate XRD analyses using calcite-aragonite mixture adjusted aragonite weight to each percentage. Ten times measurement were carried out in each aragonite ratio sample

Aragonite Weight (%)	Measurement Number	Peak intensity Aragontie (A)	Peak intensity Calcite (C)	Intensity ratio of aragonite A/ (A+C)
0	1	0	8283	-
	2	0	8036	-
	3	0	8275	-
	4	0	8088	-
	5	0	8108	-
	6	0	8094	-
	7	0	8268	-
	8	0	8040	-
	9	0	8207	-
	10	0	8271	-
10	1	90	6682	0.013
	2	85	6776	0.012
	3	90	6704	0.013
	4	74	6701	0.011
	5	96	6658	0.014
	6	84	6673	0.012
	7	97	6561	0.015
	8	75	6759	0.011
	9	83	6731	0.012
	10	78	6843	0.011
20	1	149	5697	0.025
	2	162	5734	0.027
	3	160	5468	0.028
	4	136	5685	0.023
	5	136	5446	0.024
	6	149	5577	0.026
	7	142	5711	0.024
	8	174	5485	0.031
	9	153	5614	0.027
	10	151	5505	0.027
30	1	216	4401	0.047
	2	269	4195	0.060
	3	205	4307	0.045
	4	209	4386	0.045
	5	229	4486	0.049
	6	221	4345	0.048
	7	213	4352	0.047
	8	206	4297	0.046
	9	218	4197	0.049
	10	230	4352	0.050
40	1	318	5771	0.052
	2	321	5804	0.052
	3	290	5740	0.048
	4	324	5721	0.054
	5	278	5633	0.047
	6	300	5601	0.051
	7	320	5715	0.053
	8	296	5750	0.049
	9	291	5710	0.048
	10	320	5805	0.052
50	1	300	3116	0.088
	2	315	3204	0.090
	3	304	3176	0.087

(continued)

50	4	329	3113	0.096
	5	311	3245	0.087
	6	305	3258	0.086
	7	341	3143	0.098
	8	291	3171	0.084
	9	319	3144	0.092
	10	320	3163	0.090
60	1	382	2572	0.129
	2	390	2558	0.132
	3	402	2723	0.129
	4	408	2675	0.132
	5	395	2684	0.128
	6	367	2660	0.121
	7	382	2573	0.129
	8	422	2595	0.140
	9	383	2656	0.126
	10	375	2669	0.123
70	1	512	1204	0.298
	2	528	1234	0.300
	3	480	1256	0.276
	4	504	1195	0.297
	5	476	1290	0.270
	6	499	1266	0.283
	7	473	1268	0.272
	8	493	1254	0.282
	9	456	1258	0.266
	10	438	1234	0.262
80	1	588	1589	0.270
	2	545	1431	0.276
	3	562	1578	0.263
	4	543	1565	0.258
	5	583	1521	0.277
	6	572	1504	0.276
	7	575	1555	0.270
	8	499	1543	0.244
	9	627	1555	0.287
	10	583	1531	0.276
90	1	818	1078	0.431
	2	783	1123	0.411
	3	761	1009	0.430
	4	817	1037	0.441
	5	798	1146	0.410
	6	784	1053	0.427
	7	818	1035	0.441
	8	785	1109	0.414
	9	822	1130	0.421
	10	753	1081	0.411
100	1	718	0	1
	2	717	0	1
	3	715	0	1
	4	700	0	1
	5	633	0	1
	6	708	0	1
	7	658	0	1
	8	708	0	1
	9	685	0	1
	10	688	0	1

Table 2. Results of stable isotopic measurement of carbonate chimney. Sample name corresponds to sampling point shown in Figure 2. Sample name expressed as number show the result of bulk measurement collected from the broken chimney fragments. Sampling point of #-4 is only composed of aragonite. Only the #-5 shows result of calcite and aragonite separated from the same broken fragment by staining.

Sample	$\delta^{13}\text{C}$	$\delta^{18}\text{O}$
Name	‰ (PDB)	‰ (PDB)
1	-0.86	+5.82
2	-1.07	+5.98
3	-0.92	+5.39
4	-0.94	+5.40
5	-0.53	+4.48
A-1	-0.99	+4.20
A-2	-1.68	+5.60
A-3	-2.12	+6.71
A-4	-0.59	+4.43
A-5	-0.48	+4.62
B-1	-2.12	+6.16
B-2	-1.80	+6.63
B-3	-2.06	+5.84
B-4	-1.45	+6.07
B-5	-1.40	+6.01
#-1 Aragonite	-1.17	+2.58
#-1 Calcite	-1.97	+3.48
#-2 Aragonite	-0.80	+4.15
#-2 Calcite	-0.71	+5.53
#-3 Aragonite	-1.17	+4.81
#-3 Calcite	-1.46	+5.97
#-4 Aragonite	-0.87	+5.22
#-5 Aragonite	-1.04	+4.36
#-5 Calcite	-2.24	+6.32

Table 3 Results of ^{14}C activity of carbonate chimney by LSC and AMS

Sample Name	$\Delta^{14}\text{C} \text{ ‰}$	Remarks
SURBS-50 ^a	-875.0 ± 6.5	LSC
1 Calcite	-968.8 ± 0.8	AMS
1 Aragonite	-815.7 ± 3.7	AMS
2 Calcite	-982.7 ± 0.5	AMS
2 Aragonite	-828.6 ± 2.4	AMS
3 Calcite	N.D. ^b	AMS
3 Aragonite	-847.7 ± 2.2	AMS

^a SURBS is the sample code of ^{14}C at Shizuoka University (Takahashi and Wada, 1998)

^b No Data, since carbon dioxide was pumped out accidentally during sample preparation in vacuum line

Table 4. Strontium isotopic results on calcite and aragonite

Sample Name	$^{87}\text{Sr}/^{86}\text{Sr}$	Remarks ^a
Aragonite	0.70917	Inside
Aragonite	0.70911	Outside
Calcite	0.70669	Inside
Calcite	0.70679	Outside

^a Inside and outside shows the sampling points of each mineral. Inside means near the center part and outside means near the outer wall of carbonate chimney. Calcite and aragonite was separated from the same sampling point.

Table 5. The $^{87}\text{Sr}/^{86}\text{Sr}$ ratio of modern seawater.

Phase	$^{87}\text{Sr}/^{86}\text{Sr}$		$^{87}\text{Sr}/^{86}\text{Sr}$ corr.	Ref. ^a
	Sample	NBS 987		
Carbonate				
Shell and sediments (n = 41)	0.709070 ± 40	0.71014	0.709205 ^b	1
Shells (n = 18)	0.709234 ± 9	0.71031	0.709199	2
Foraminifera (n = 25)	0.709238 ± 29	0.710275	0.709238	3
mean value (n = 84)			0.709211	
Seawater				
IAPSO standard (N.E. Atlantic				
ocean) (N = 23)	0.709187 ± 38	0.71026	0.709202	4
Arabian Gulf (N = 1)	0.70911	0.71014	0.709245 ^b	1
modern seawater (N = 9)	0.709198 ± 20	0.710220	0.709253 ^b	5
NE continental shelf of USA (N = 1)	0.709200	—	0.709266	6
mean value (n = 4)			0.709241 ^b	

^aRef., 1 = Burke et al. (1982); 2 = DePaolo and Ingram (1985); 3 = Palmer and Elderfield (1985); 4 = Elderfield and Greaves (1981); 5 = Hess et al. (1986); 6 = Staudigel et al. (1985); ^bCorr., normalized to NBS 987 = 0.710275; n =, number of samples; N =, number of replicates, after from Elderfield (1986)

Table 6. Composition of interstitial water from core of site 780, ODP leg125 at the Conical Seamount (Mottle, 1992).

Cations	Concentration (mmol/l)	Electric charge (meq/l)	Anions	Concentration (mmol/l)	Electric charge (meq/l)
Na ⁺	420	420	Cl ⁻	280	280
K ⁺	15	15	SO ₄ ²⁻	45	90
Li	0	0	B	4	4
Mg ²⁺	0	0	NH ₃	0.250	0.250
Ca ²⁺	0	0	Br	0.0006	0.0006
Sr ²⁺	0.010	0.010			
Ba ²⁺	0	0			
Mn ²⁺	0	0			
	Total	435		Total	374

Table 7. Isotopic fractionation of a coexisting aragonite and calcite. Sample name corresponds to sampling point shown in Figure 11, except for #-5. Sampling point of #-4 is not added because this point is only composed of aragonite. Sample name of #-5 shows the bulk value collected from the broken chimney fragments.

Sample	$\delta^{13}\text{C}$ (aragonite-calcite)	$\delta^{18}\text{O}$ (aragonite-calcite)
Name	‰ (PDB)	‰ (SMOW)
#-1	0.80	-0.93
#-2	-0.09	-1.38
#-3	0.29	-1.21
#-5	1.20	-2.03

Table 8. Estimate temperature and oxygen isotopic ratio of venting fluid

Sample ^a	$\delta^{18}\text{O}_{\text{carbonate}}$	Temp. ^b	$\delta^{18}\text{O}_{\text{venting fluid}}^{\text{c}}$
Name	(‰ SMOW)	(°C)	(‰ SMOW)
#-1 Aragonite	33.46	3.7	-0.59
#-1 Calcite	34.45	0.2	0.37
#-2 Aragonite	35.09	-2.1	0.98
#-2 Calcite	36.56	-7.0	2.41
#-3 Aragonite	35.75	-4.3	1.62
#-3 Calcite	37.02	-8.5	2.85
#-4 Aragonite	36.18	-5.8	2.04

^a Sample name corresponds to Table 2 and Figure 13

^b Precipitation temperature were calculated from oxygen isotopic values of carbonate chimney, using the equation given by O'Neil et al. (1969) and Tarutani et al. (1969)

^c Oxygen isotopic values of fluid were calculated from which carbonate chimney was precipitated at 1.5°C, using the equation given by O'Neil et al. (1969) and Tarutani et al. (1969)

Table 9. Carbon and oxygen isotopic values of carbonate cements included in matrix. Carbonate mineral phase of cements was measured by X-ray diffractometer.

Sample Name	$\delta^{13}\text{C}$ ‰ (PDB)	$\delta^{18}\text{O}$ ‰ (PDB)	Carbonate Mineral
010915-1 P.2	-30.69	-4.94	Calcite
010915-1 P.3	-49.32	+1.59	Calcite
010915-1 P.4	-51.36	+0.14	Calcite
010915-1 P.5	-42.09	-3.10	Calcite
010915-1 P.7	-53.21	+1.32	Calcite